NOAA Technical Report ERL 328-AOML 17

U.S. DEPARTMENT OF COMMERCE
NATIONAL OCEANIC AND ATMOSPHERIC ADMINISTRATION
Environmental Research Laboratories

Examination of Water Movement in Massachusetts Bay

DENNIS A. MAYER

BOULDER, COLO.
JANUARY 1975

U.S. DEPARTMENT OF COMMERCE
Frederick B. Dent, Secretary

NATIONAL OCEANIC AND ATMOSPHERIC ADMINISTRATION
Robert M. White, Administrator
ENVIRONMENTAL RESEARCH LABORATORIES
Wilmot N. Hess, Director

NOAA TECHNICAL REPORT ERL 328-AOML 17

Examination of Water Movement in Massachusetts Bay

DENNIS A. MAYER

BOULDER, COLO.
January 1975

For sale by the Superintendent of Documents, U. S. Government Printing Office, Washington, D. C. 20402

DISCLAIMER

The Environmental Research Laboratories do not approve, recommend, or endorse any proprietary product or proprietary material mentioned in this publication. No reference shall be made to the Environmental Research Laboratories or to this publication furnished by the Environmental Research Laboratories in any advertising or sales promotion which would indicate or imply that the Environmental Research Laboratories approve, recommend, or endorse any proprietary product or proprietary material mentioned herein, or which has as its purpose an intent to cause directly or indirectly the advertised product to be used or purchased because of this Environmental Research Laboratories publication.

CONTENTS

EXAMINATION OF WATER MOVEMENT IN MASSACHUSETTS BAY

Dennis A. Mayer

ABSTRACT

NOMES (New England Offshore Mining and Environmental Study) was conducted by the National Oceanic and Atmospheric Administration (NOAA) and the State of Massachusetts to determine what impact offshore mining of sand and gravel would have on the chemistry and biology of Massachusetts Bay. Specifically, the physical oceanography part of the study was intended to predict how material, in this case the dredge plume fines (d<100 m), would be dispersed. Water movement in Massachusetts Bay is characterized by great spatial and temporal variability. During the month that current meter and drogue measurements were taken, the major feature of the variability was the existence of a strong north-south current shear zone. The mean motions near shore (≈10 km) were predominantly northward; and in less than 10 km to the east, the motions were mostly southward. A prediction, therefore, of how material would be dispersed if it were introduced in the water column would depend largely on where and when it was introduced. In addition, a comparison of drogue and current meter data points out the hazards of depending exclusively on either Lagrangian or Eulerian measurements in describing how material would be dispersed in Massachusetts Bay.

1. INTRODUCTION

NOMES was conducted by NOAA and the State of Massachusetts to determine what impact offshore mining of sand and gravel would have on the chemistry and biology of Massachusetts Bay. Specifically, the physical oceanography part of the study was intended to predict how the dredge plume fines (d<100 m) would be dispersed. A four-pronged assault was launched on the problem in May 1973; on May 24th and 25th, eight current meter stations with a total of 28 current meters were deployed by EG&G and the Atlantic Oceanographic

and Meteorological Laboratories (AOML). These remained in place until June 25th. Of the 28 current meters deployed, 21 produced full record lengths. The last three phases began on June 11th when four drogues were launched in conjunction with a water-tracing study. The drogues were tracked for 3 days, and the water-tracing study continued for 7 additional days. This report is devoted to the current meter and drogue data.

2. DESCRIPTION OF THE EXPERIMENT

Eight current meter stations were deployed on May 24th and 25th for 1 month. Of the 28 current meters, 10 were Aanderaa and 18 were photogeodynes deployed by EG&G (Magas, 1973). Current meter stations are shown in figure 1. Table 1 provides the necessary mooring data such as sensor depths for each of the stations. No data were recorded from station 3. All current meters that returned useful records are indicated in table 1; those that did not are excluded. Wind data were obtained from the Boston Lightship located near station A.

2.1 Eulerian Measurements

The data sets were divided into three levels: upper, middle, and lower measurements; 1, 2, and 3, respectively. These three levels are indicated in table 2; statistics are also given. The statistics tabulated include monthly mean velocity components (the larger ones are plotted in fig. 1)

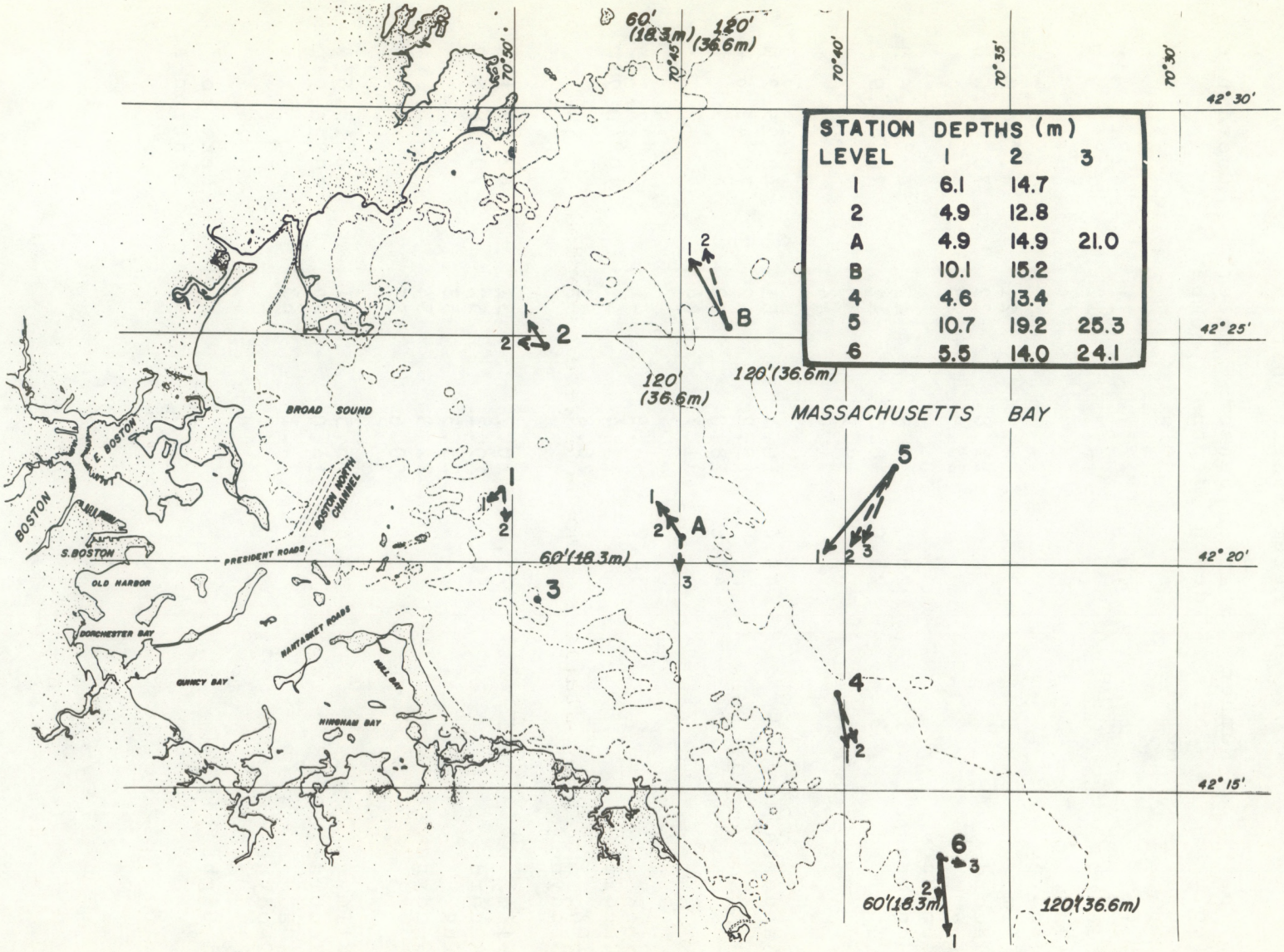

Figure 1. Monthly mean current vectors.

Table 1.
Current Meter Mooring Data

Sta.	Type of sensor	Number of meters	Station depth (m)	Sensor depths (m)	Meter number	Coordinates
1	Film Recording Geodyne	2	19.8	6.1 14.7	11 12	42°21.6'N 70°50.3'W
2	Film Recording Geodyne	3	33.2	4.9 12.8 25.9	21 22 23	42°24.8'N 70°49.0'W
A	Aanderaa	1 3	29.9 25.0	4.9 8.5 14.9 21.0	A1 A2 A3 A4	42°20.6'N 70°44.9'W
B	Aanderaa	2 2	49.4 47.8	10.1 15.2 18.0 31.7	B1 B2 B3 B4	42°25.2'N 70°43.6'W
4	Film Recording Geodyne	3	34.2	4.6 13.4 26.8	41 42 43	42°17.1'N 70°40.2'W
5	Film Recording Geodyne	5	71.4	10.7 19.2 25.3 32.3 50.6	51 52 53 54 55	42°22.1'N 70°38.5'W
6	Film Recording Geodyne	3	31.4	5.5 14.0 24.1	61 62 63	42°13.6'N 70°36.9'W
Wind Lightship						Next to station A

Table 2.

Statistics of 40-Hr Low- and High-passed Time Series

Sta.	Meter number	Level number	Record length number of points Δt=1.0 hr	cm/s mean north component	cm/s mean east component	HPV high-passed variance	LPV low-passed variance	Squared mean	Ratio of HPV to total variance	Ratio of total variance to squared mean
1	Δ11	1	605	-0.84	-0.80	183.4	80.7	1.4	0.69	195.6
	Δ12	2	592	-2.51	0.35	92.4	17.6	6.4	0.84	17.1
2	21	1	586	1.87	-1.33	120.7	57.0	5.3	0.68	33.7
	22	2	586	0.42	-1.92	186.1	31.9	3.9	0.85	55.9
	*23	3	303	-3.42	7.30	80.1	11.3	65.0	0.88	1.4
A	A1	1	615	2.70	-2.03	125.0	106.0	11.4	0.54	20.3
	A2	1	615	3.42	-3.19	232.3	79.8	21.9	0.74	14.3
	A3	2	611	1.76	-1.52	154.4	46.2	5.4	0.77	37.2
	A4	3	611	-2.45	0.05	116.3	7.4	6.0	0.94	20.6
B	B1	1	615	5.04	-2.89	116.5	42.9	33.8	0.73	4.7
	B2	2	615	5.56	-1.27	42.6	43.7	34.1	0.49	2.5
	B3	2	611	4.43	-1.17	90.1	23.7	21.0	0.79	5.4
	B4	3	611	1.79	-0.48	85.0	9.4	3.4	0.90	27.8
4	41	1	592	-3.48	0.96	228.0	156.2	13.0	0.59	30.0
	42	2	592	-3.47	1.42	188.6	94.6	14.0	0.67	21.0
	*43	3	158	5.98	0.12	266.6	26.2	35.8	0.91	8.2
5	51	1	592	-6.12	-5.52	171.0	106.0	67.9	0.62	4.1
	52	2	592	-6.12	-3.47	97.5	50.7	49.5	0.66	3.0
	53	3	592	-5.49	-2.33	68.4	42.0	35.6	0.62	3.1
	54	3	600	-5.97	-3.67	182.6	108.0	49.1	0.63	5.9
	Δ55	3	605	-3.22	-0.42	76.7	42.5	10.5	0.64	11.35
6	61	1	594	-5.49	0.74	172.8	148.9	30.7	0.54	10.5
	*62	2	535	-3.13	0.13	224.4	120.1	9.8	0.65	35.2
	63	3	594	-0.60	1.75	104.3	23.5	3.4	0.82	37.4

Δ Record too long.
* Record too short.

and the high-passed variance, low-passed variance, and squared mean. The data sets were partitioned into low and high frequency bands. Forty hours was selected as the period separating low and high frequency processes; thus, 40-hr hp data contain all high frequency events such as inertial and tidal frequencies, and 40-hr lp data contain all events with periods greater than 2 days or those usually associated with synoptic meteorological events. The variances computed are the sum of the squares of the variances of the velocity components for each time series--40 hr lp and 40-hr hp. In addition, the ratio of high-passed variance (HPV) to total variance and the ratio of total variance to the squared mean are also given. The latter ratio is of particular interest in analyzing the dispersion of materials.

2.2 Lagrangian Measurements

Three drogues were deployed, beginning at 1100 on June 11th and tracked for over 2 days. The drogues were developed by the R. M. Parsons Laboratory at Massachusetts Institute of Technology (MIT). Only the 7- and 12-m drogue data were used for comparison with the current meter data because not enough data from the stations at the lower level (3) were available. The 7- and 12-m drogues correspond to levels 1 and 2, respectively.

3. MEAN MOTIONS

The larger mean current vectors at various levels for all the stations are shown in figure 1. These means should be interpreted with caution as they reflect an average of about a month. With only this much data and such great variability, these means are probably not well determined and would fluctuate from month to month. To show how variable the motions are, we can look at the ratio of the total variance to the mean squared (table 2). This quantity varies from about 3 to 200. Data from station 1 show almost zero mean with a very large variance. Station 5, on the other hand, shows small values ranging from 3 to about 11. This shows that a consistently large mean flow existed for the duration of the experiment for station 5. The flow at all levels for station 5 is consistently to the southwest, whereas most other means appear to parallel the isobaths. At every other station, the flow seems to be influenced by the boundaries. An interesting feature of the vertical structure is seen in the record for the near bottom meter (A4) at station A. Here the current is to the south, whereas the upper three sensors at station A show a mean northerly flow.

3.1 Direction Data

Histograms in polar form summarize the direction data for the 40-hr hp time series for all three levels in figures 2 to

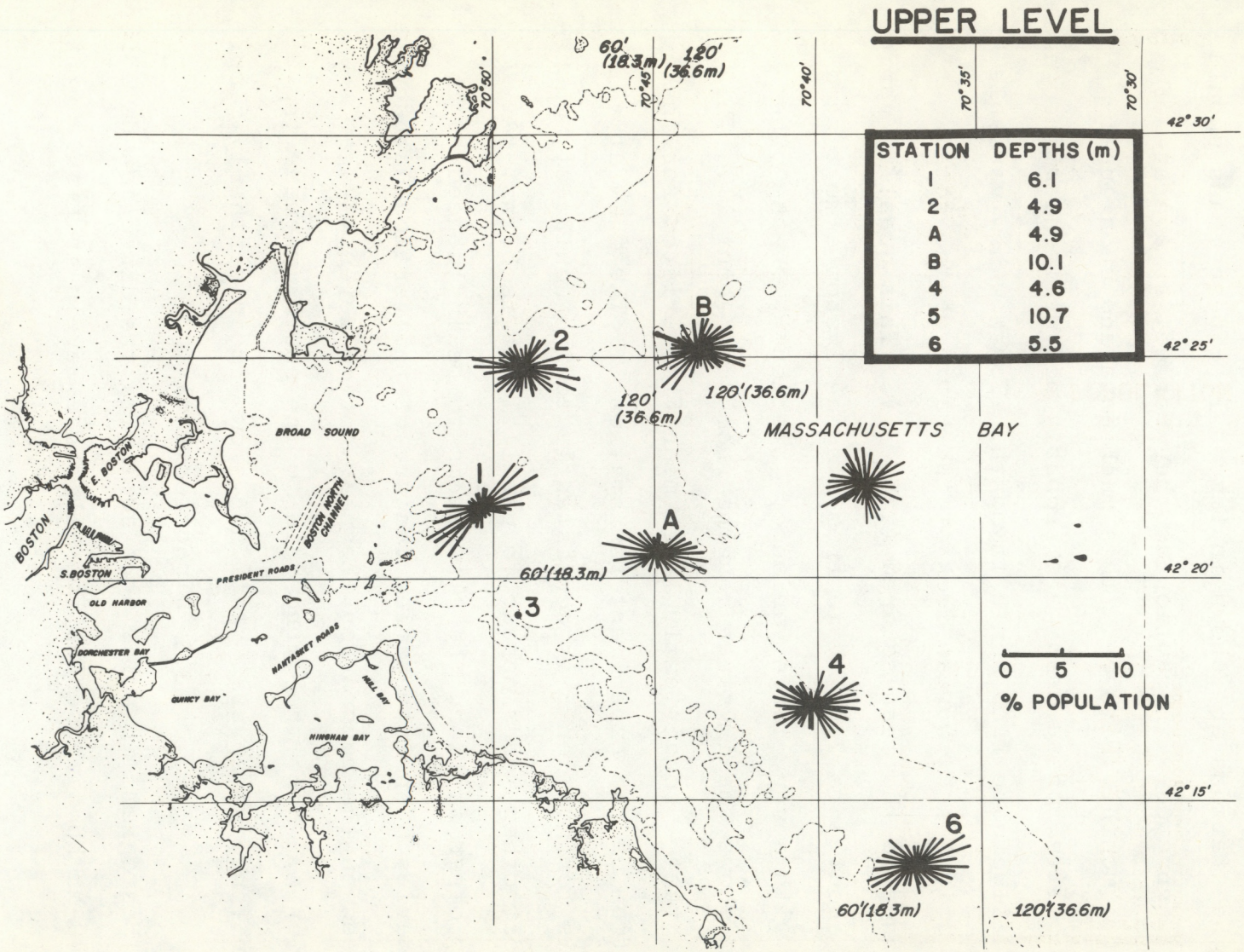

Figure 2. Current roses of percent population for upper level meters.

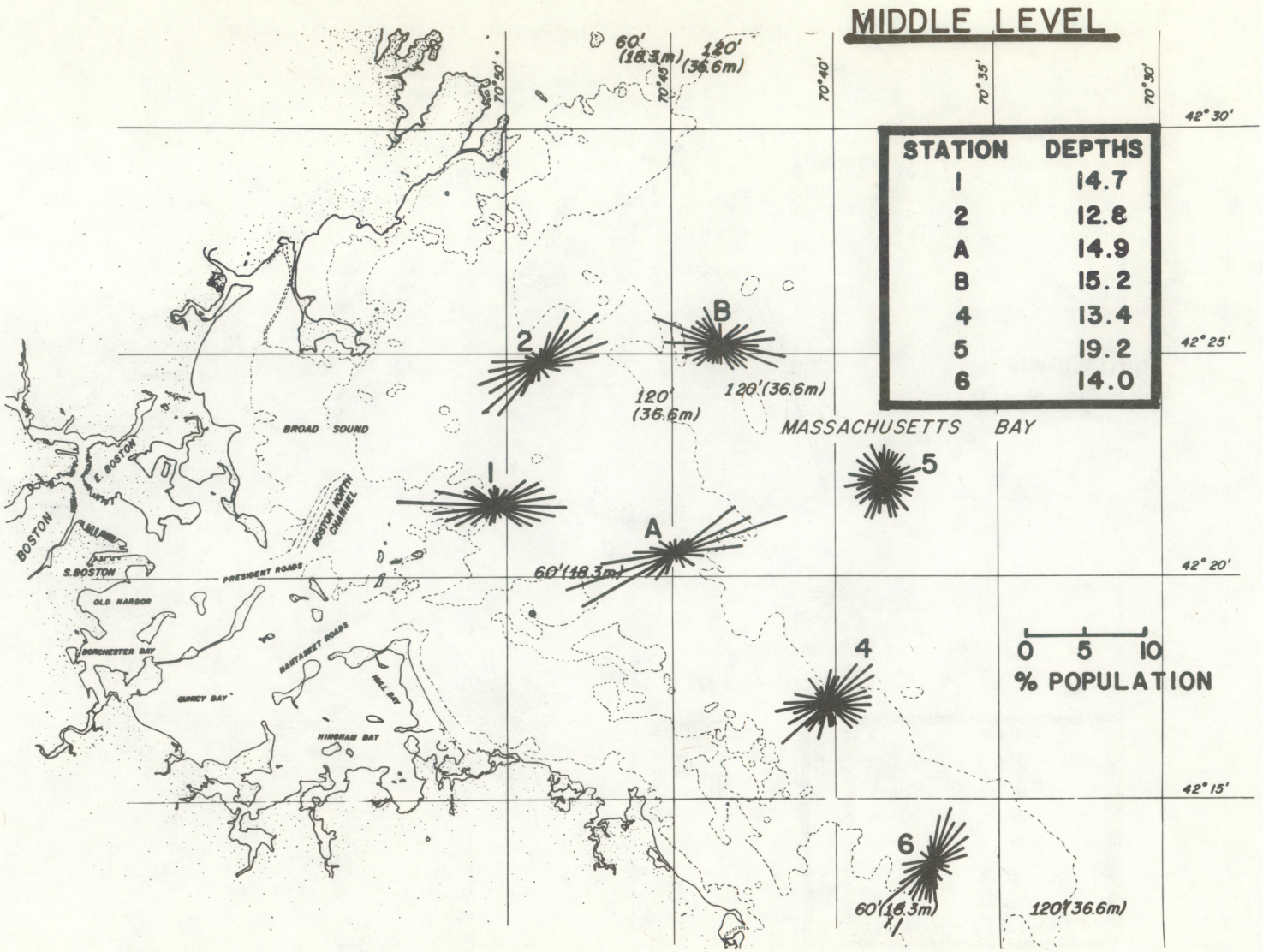

Figure 3. Current roses of percent population for middle level meters.

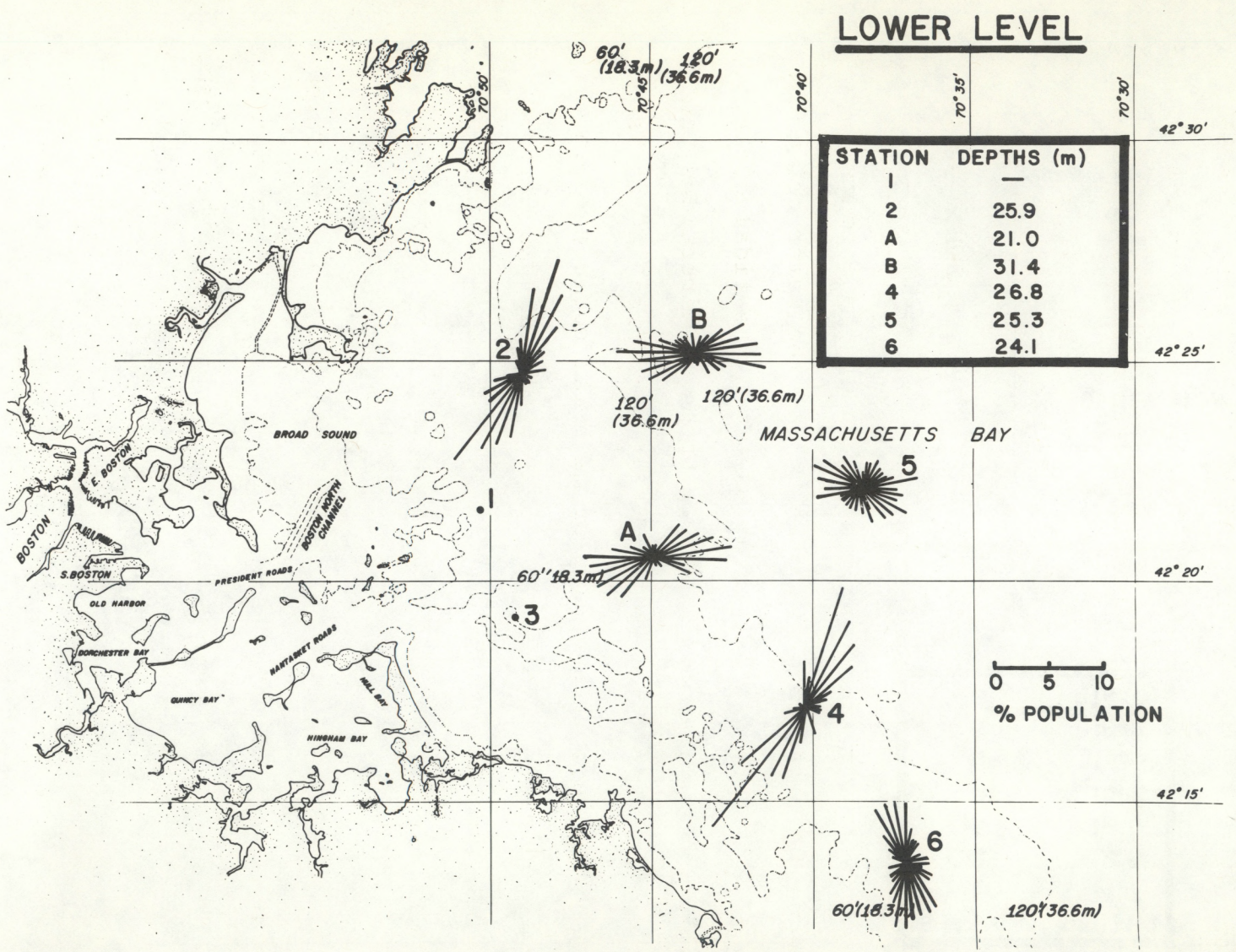

Figure 4. Current roses of percent population for lower level meters.

4. The histograms display the preferred directions of the water motion as the frequency distribution of currents, partitioned into 10° increments, where the length of each line represents the percentage of the total record length occupying that direction segment. Frequency distributions change significantly with depth. Level 1 has fairly homogeneous distributions of currents, except for station 1. Levels 2 and 3 show that materials would be transported in a preferred southwest and northeast direction. Of course, there is no phase information contained in these roses. This means that material introduced into the water column at the same place, but at different times in the tidal cycle, could be transported in completely opposite directions; and if the spatial variation of currents is as great as it is in Massachusetts Bay, then a slug of material could move in almost any direction, depending on the time it was introduced into the water column. This will be brought up again when an explanation of the drogue tracks is presented.

3.2 Vector Time Series of 40-Hr Lp Data

The low frequency content of the data is best displayed as a stick diagram. These are shown in figures 5 through 11 for all stations, and the time interval is every 6 hr. Here it can be seen that stations 4, 5, and 6 differ distinctly from the other stations in that the flow is predominantly southward. Also the low frequency motions of these three

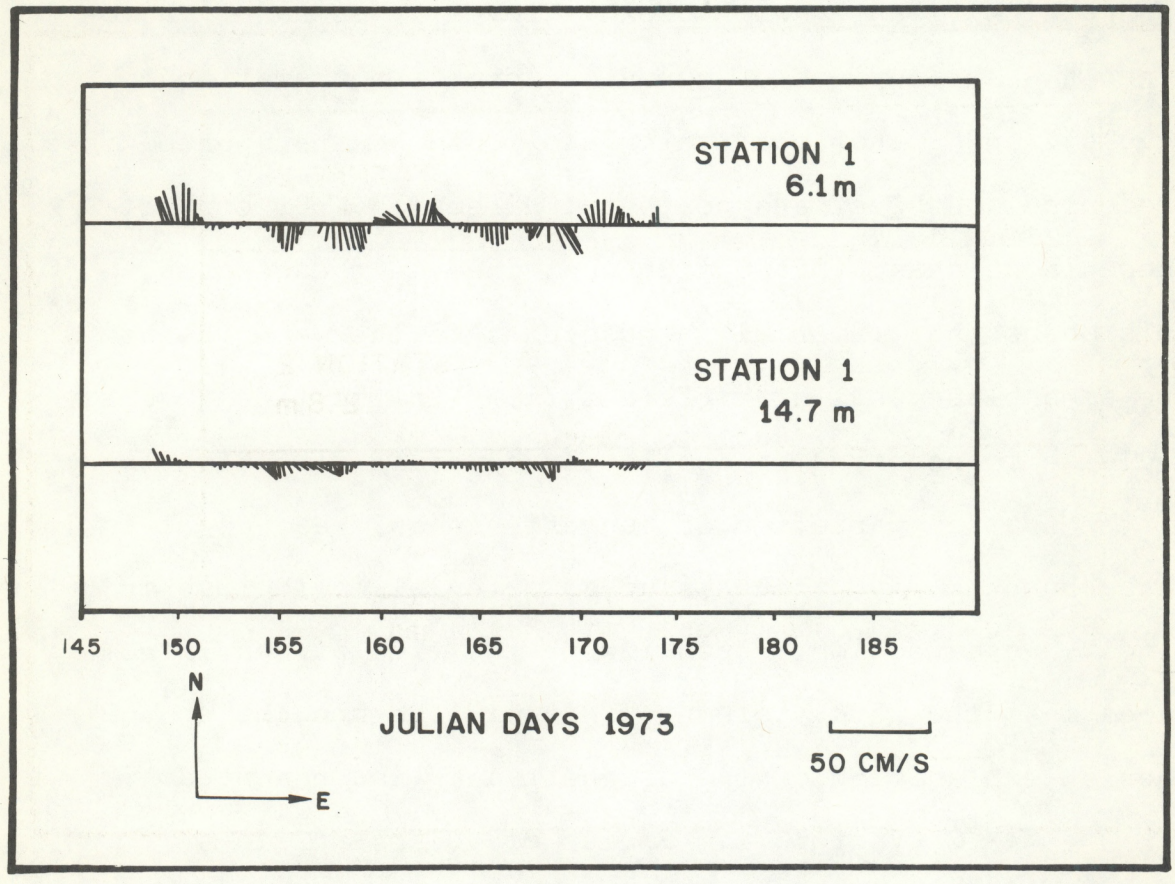

Figure 5. Vector time series of 40-hr lp data for station 1 (Δt = 6 hr).

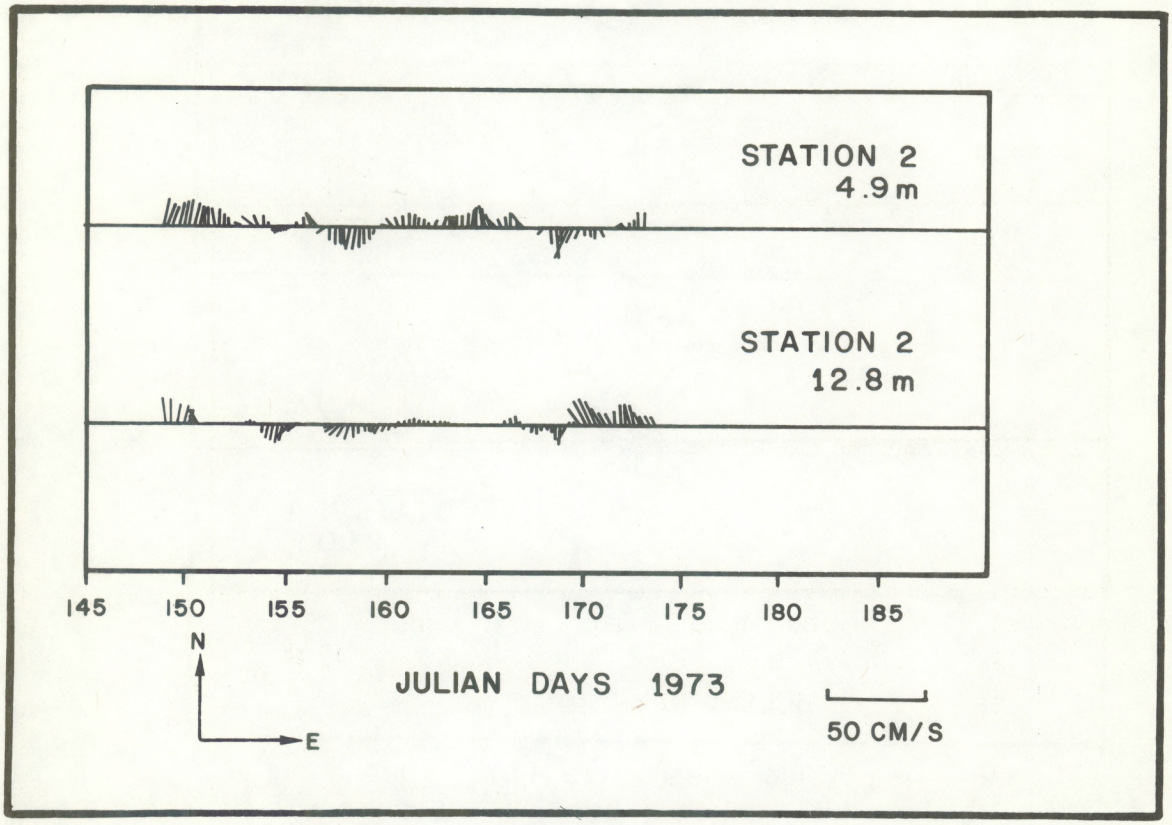

Figure 6. Vector time series of 40-hr lp data for station 2 (Δt = 6 hr).

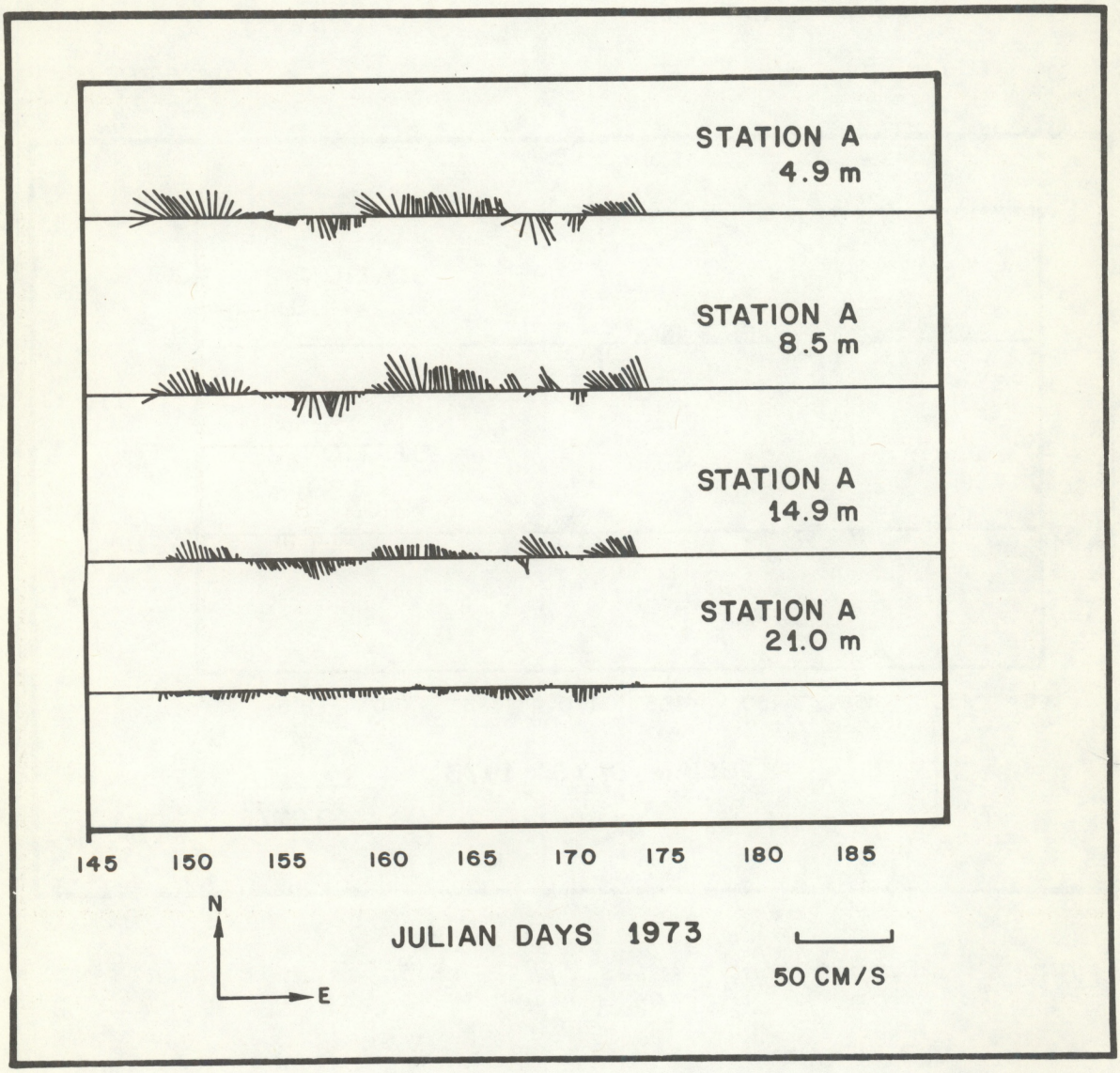

Figure 7. Vector time series of 40-hr lp data for station A (Δt = 6 hr).

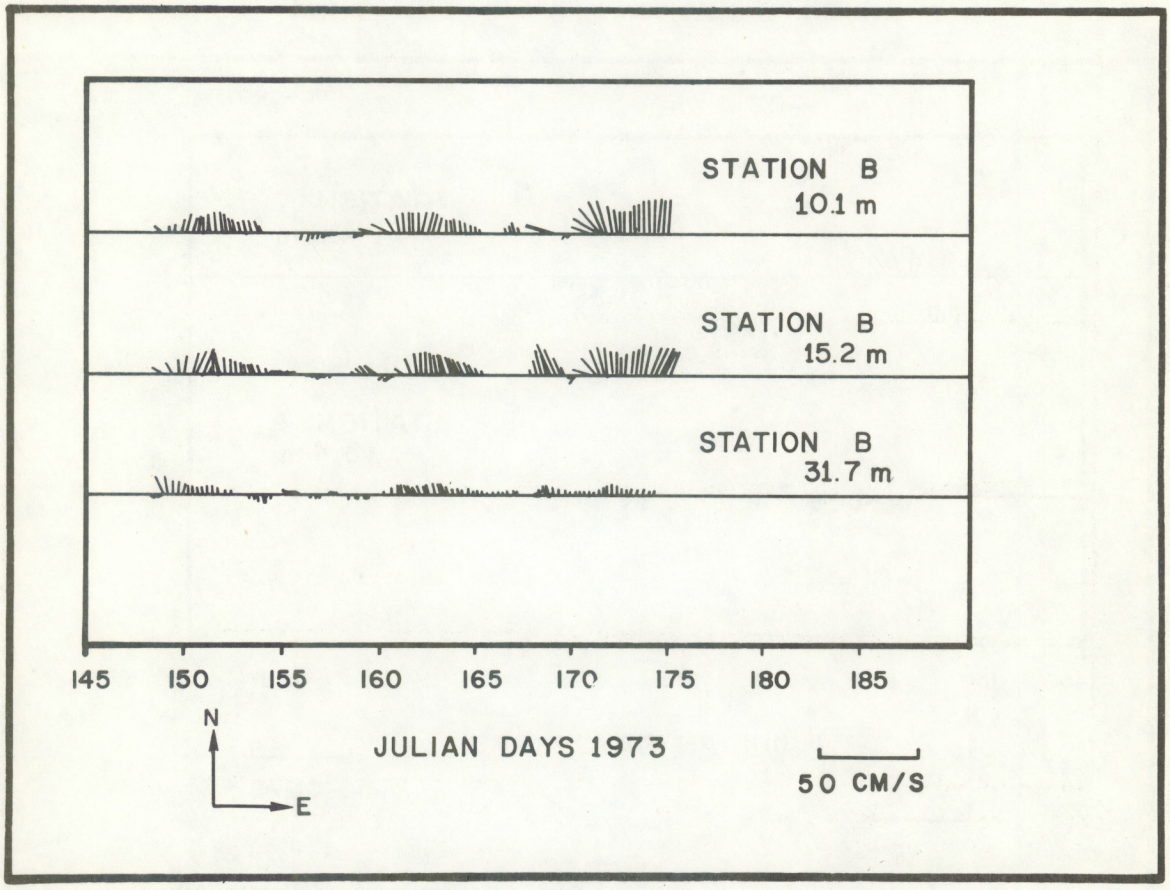

Figure 8. Vector time series of 40-hr lp data for station B (Δt = 6 hr).

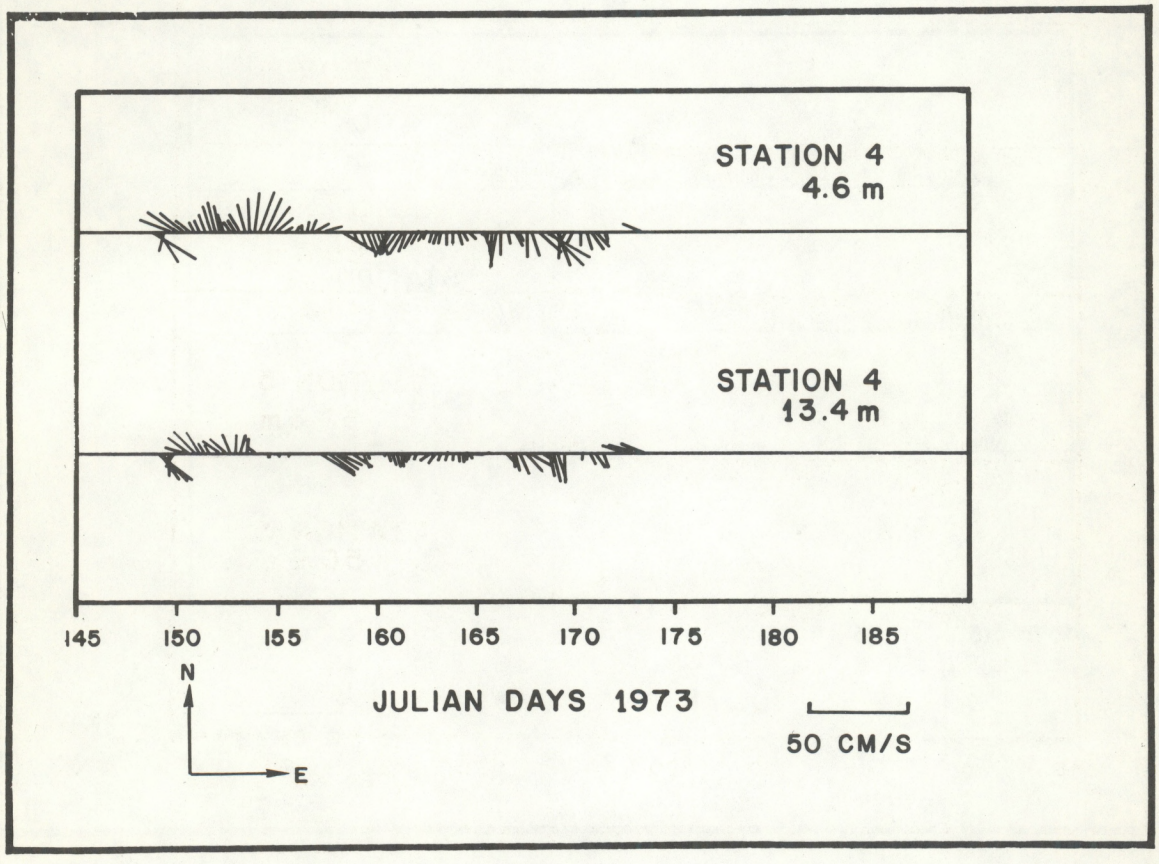

Figure 9. Vector time series of 40-hr lp data for station 4 (Δt = 6 hr).

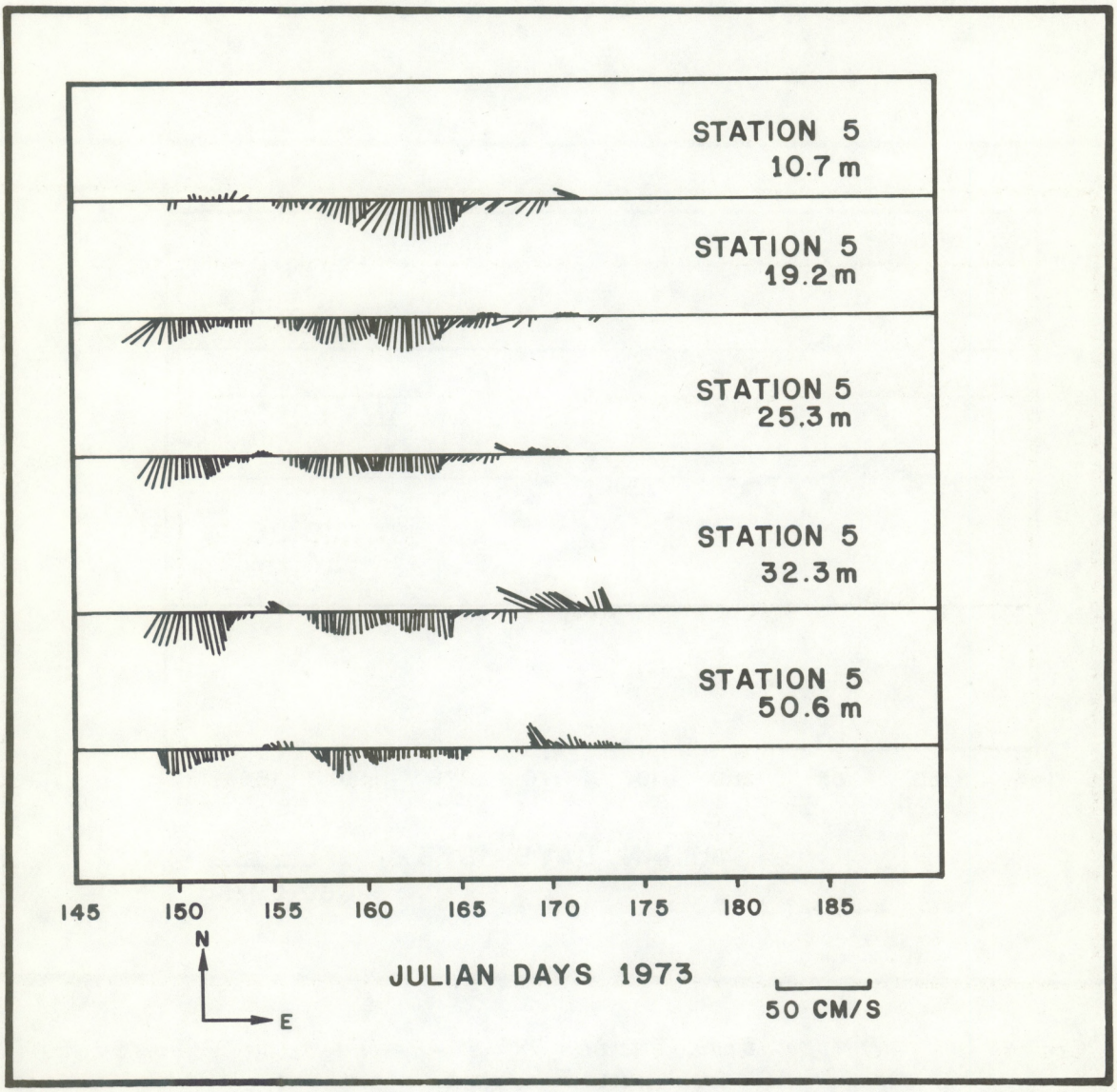

Figure 10. Vector time series of 40-hr lp data for station 5 (Δt = 6 hr).

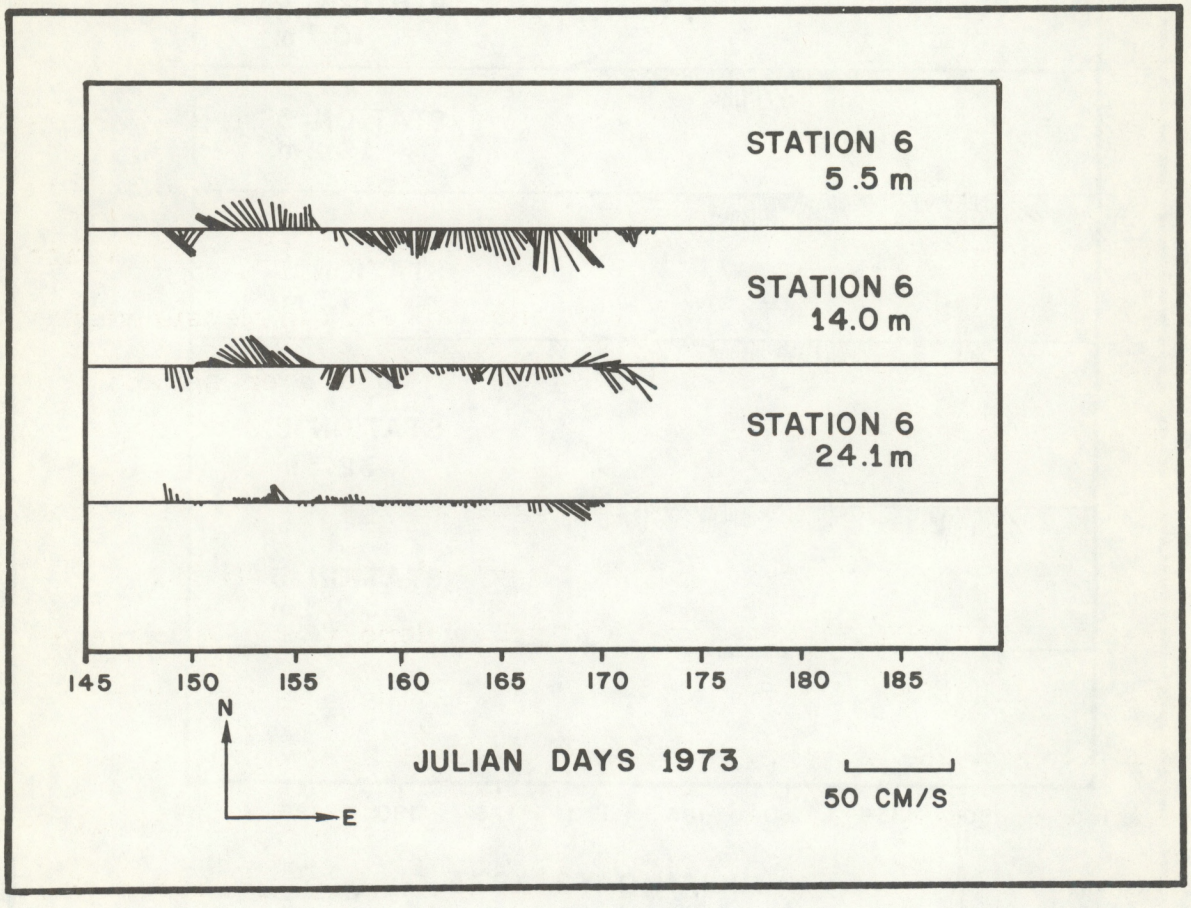

Figure 11. Vector time series of 40-hr lp data for station 6 (Δt = 6 hr).

stations appear to be as much as 180° out of phase with stations 1, 2, A, and B for more than one-half the record length. The flow at the 21-m sensor at station A is also southward. It is apparent that there is a great spatial variability in the current field, with scale length less than 10 km. The major feature of this variability is the existence of a strong north-south current shear zone where strong northerly currents at station A change to strong southerly currents at station 5. This feature can greatly complicate any comparison between Eulerian and Lagrangian measurements, unless the Lagrangian water-tracing is done over several tidal cycles.

3.3 Temperature Time Series

The only temperature data obtained were from the Aanderaa meters at stations A and B. Here the raw temperature data (fig. 12 and 13) show decreasing fluctuations with depth as expected, and both stations also show a significant temperature jump at all levels except for the 31.7-m sensor at station B. The jump begins roughly on Julian Day 168 or June 17, 1973. The increase in temperature at all levels above 20 m is roughly 5°C. This does not appear to be associated with any meteorological events because the progressive vector diagram in figure 14 of the wind, as observed by the lightship, shows nothing unusual occurring on that date. What may be significant, however, is that, from figures 5

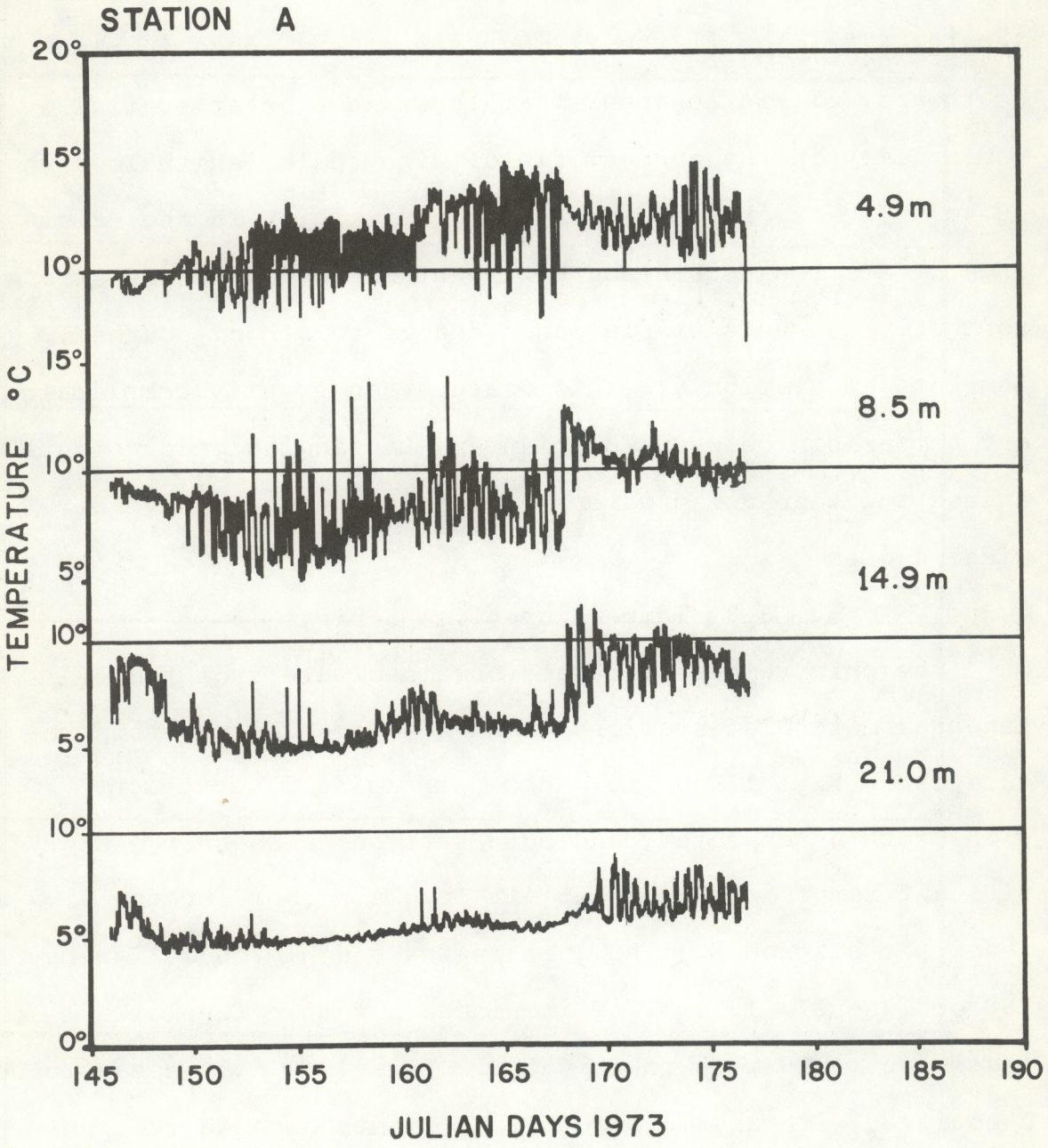

Figure 12. Temperature data from station A.

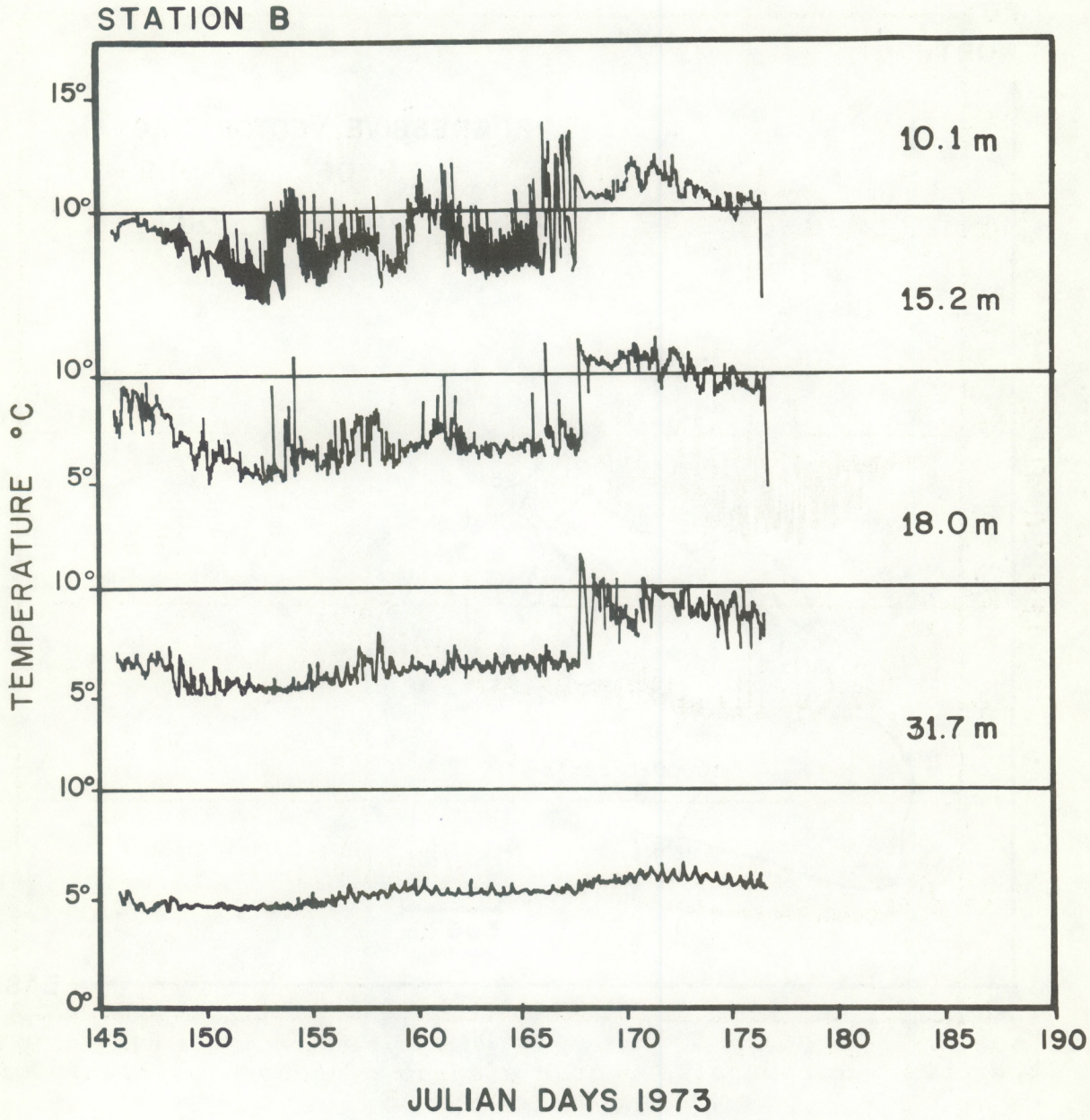

Figure 13. Temperature data from station B.

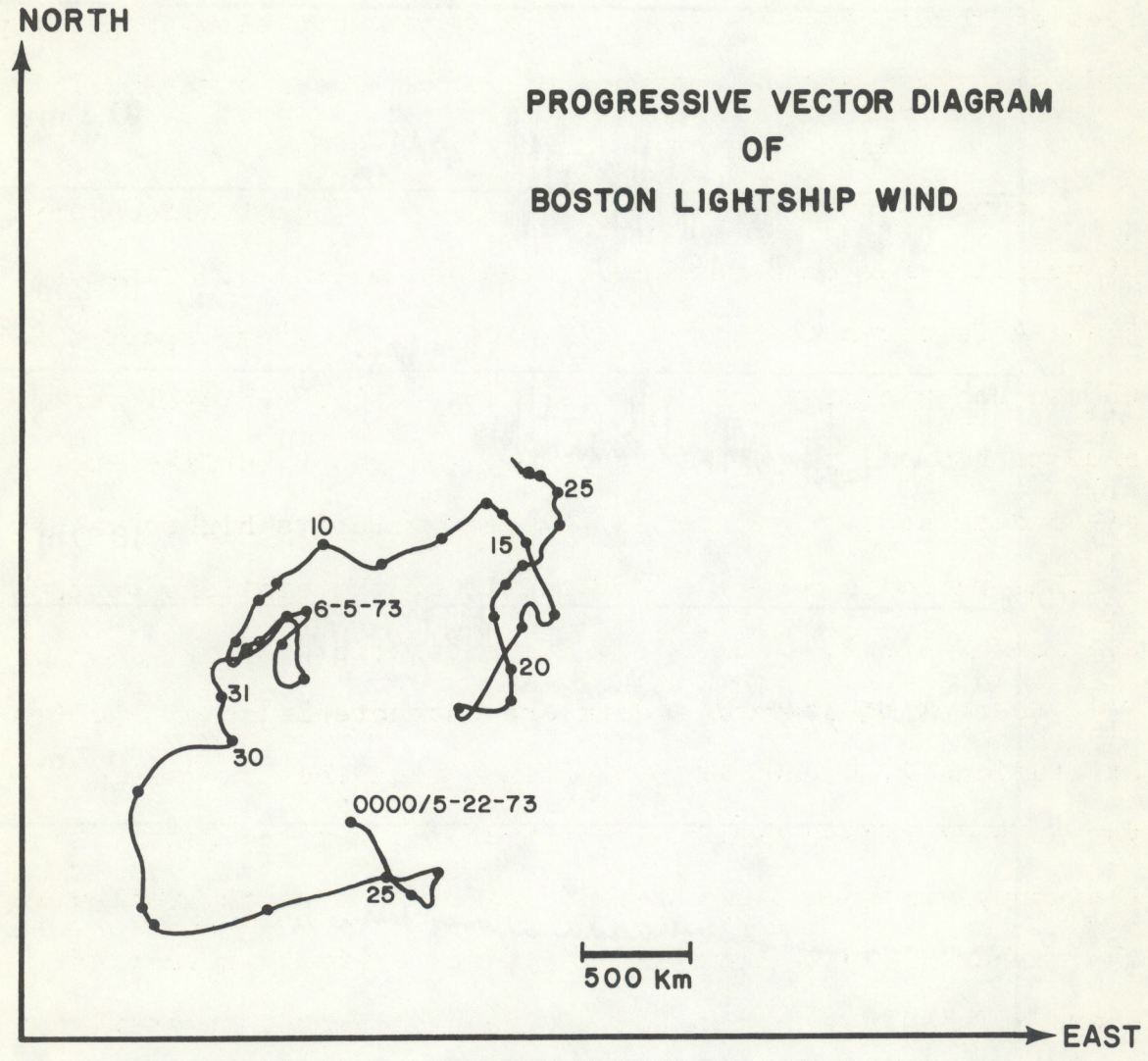

Figure 14. Progressive vector diagram of Boston Lightship wind.

through 11, stations 4 and 6 show unusually strong southerly flow, station 5 shows strong westerly flow, and station A has some unusual vertical current structure, that is, southerly flow at the surface and a variable structure below. This may indicate the transport onshore of warmer oceanic water.

3.4 Spectra of Current Meter Data

Comparison of spectra of the north and east components of velocity for mean surface and bottom meters at stations 5 and A is shown in figures 15 through 18. These spectra were chosen because station 5 with its low ratios of total variance to squared mean is, except for station B, unlike the other data sets. Station A, however, with its higher values of this ratio is more characteristic of the stations west of stations 5 and B, at least in its energetics.

Spectra of station A data are characteristic of spectra at stations 2, 4, and 6. This means that the low-passed variance decreased regularly with depth, but the high frequency variance sometimes increases with depth, reflecting the rather vigorous inertial and tidal activity nearer the shore. This feature can be seen in the spectra of station A in figures 15 and 16 where the high frequency portion of the spectra for the upper and lower sensors is quite close in magnitude. Station 5, on the other hand, shows that both low and high frequency variance decrease fairly uniformly with depth. This can be seen in table 2 by looking at the ratio

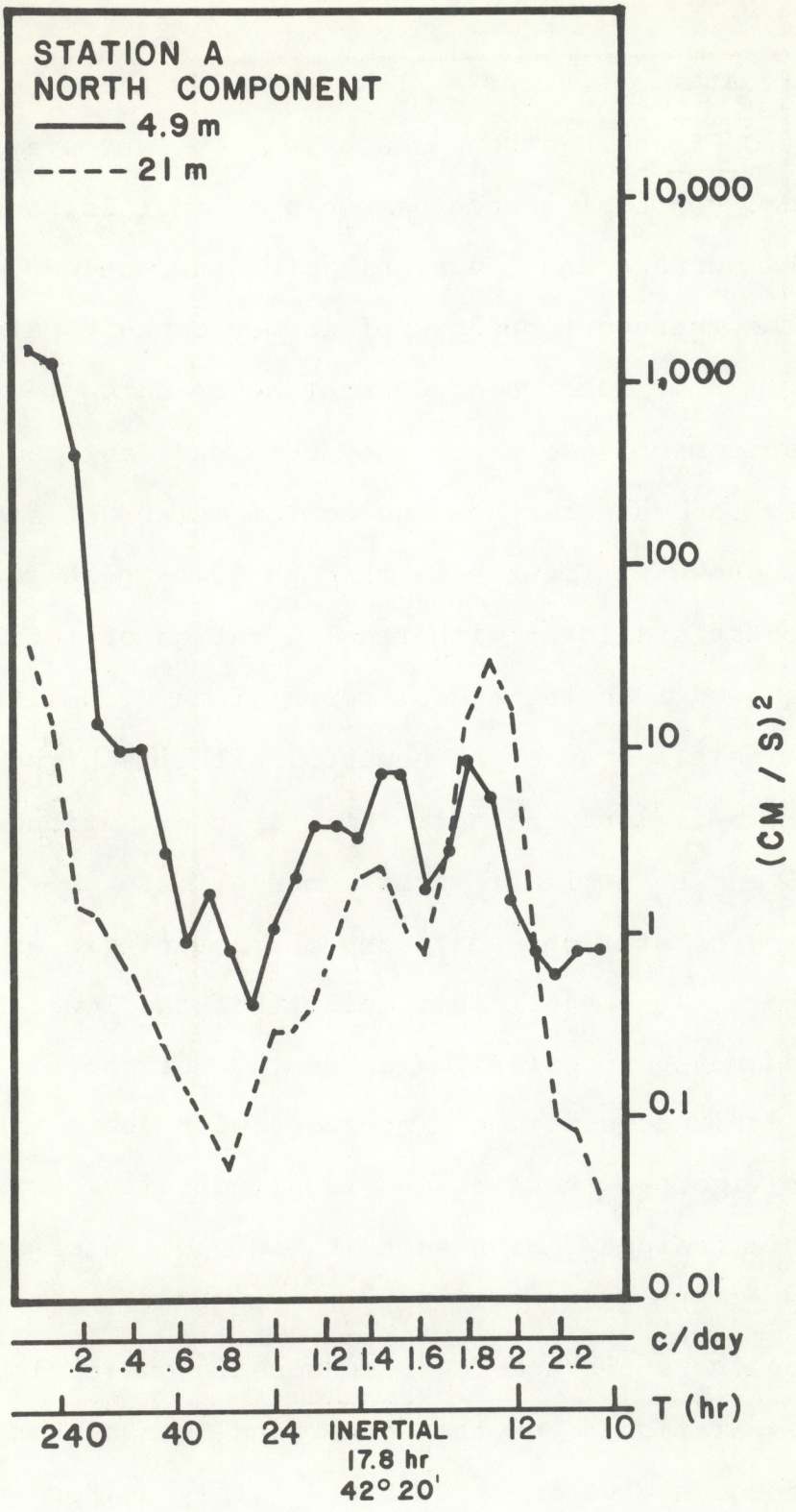

Figure 15. Spectra of north component of current for station A at 4.9 and 21 m.

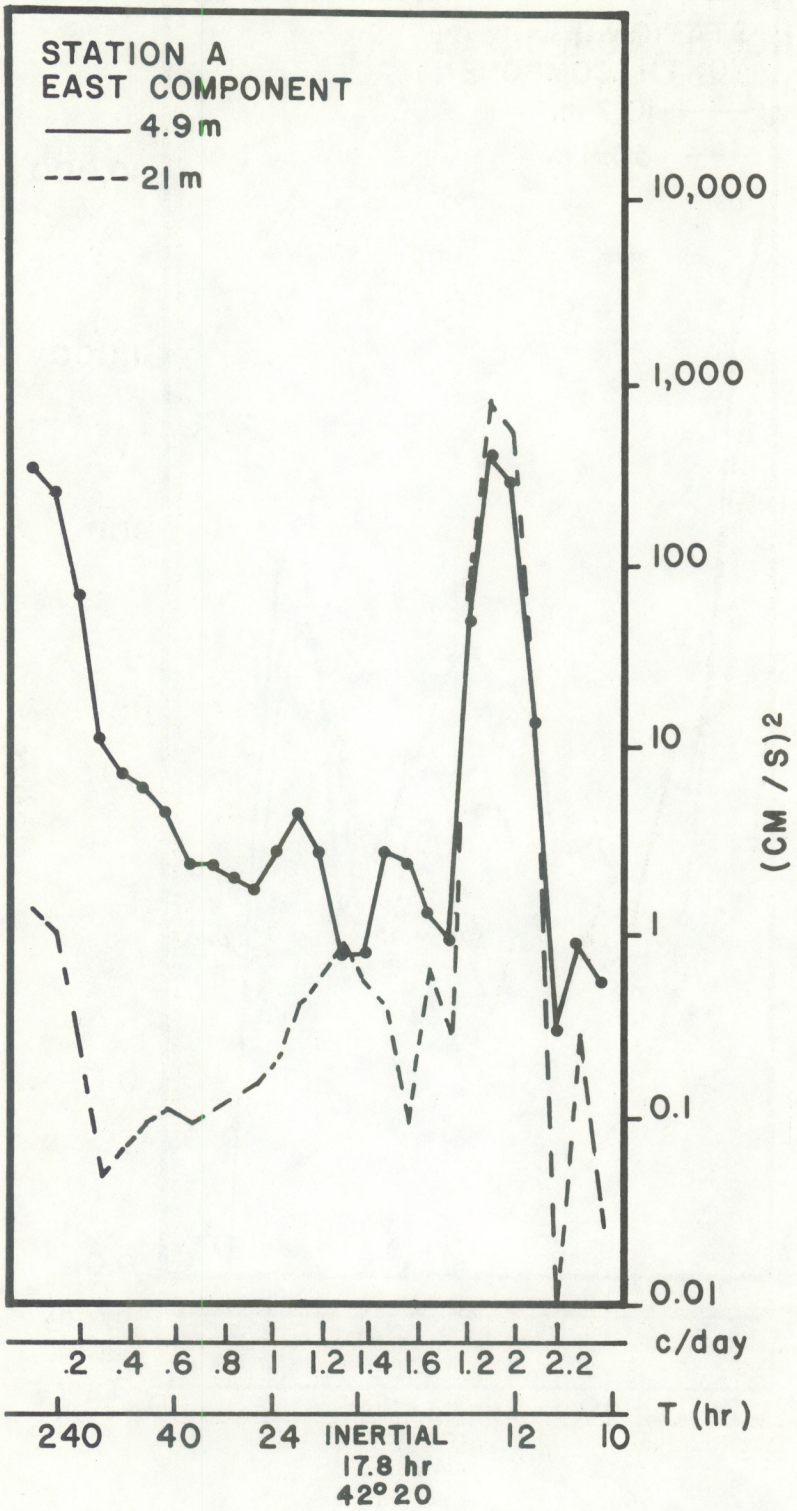

Figure 16. Spectra of east component of current for station A at 4.9 and 21 m.

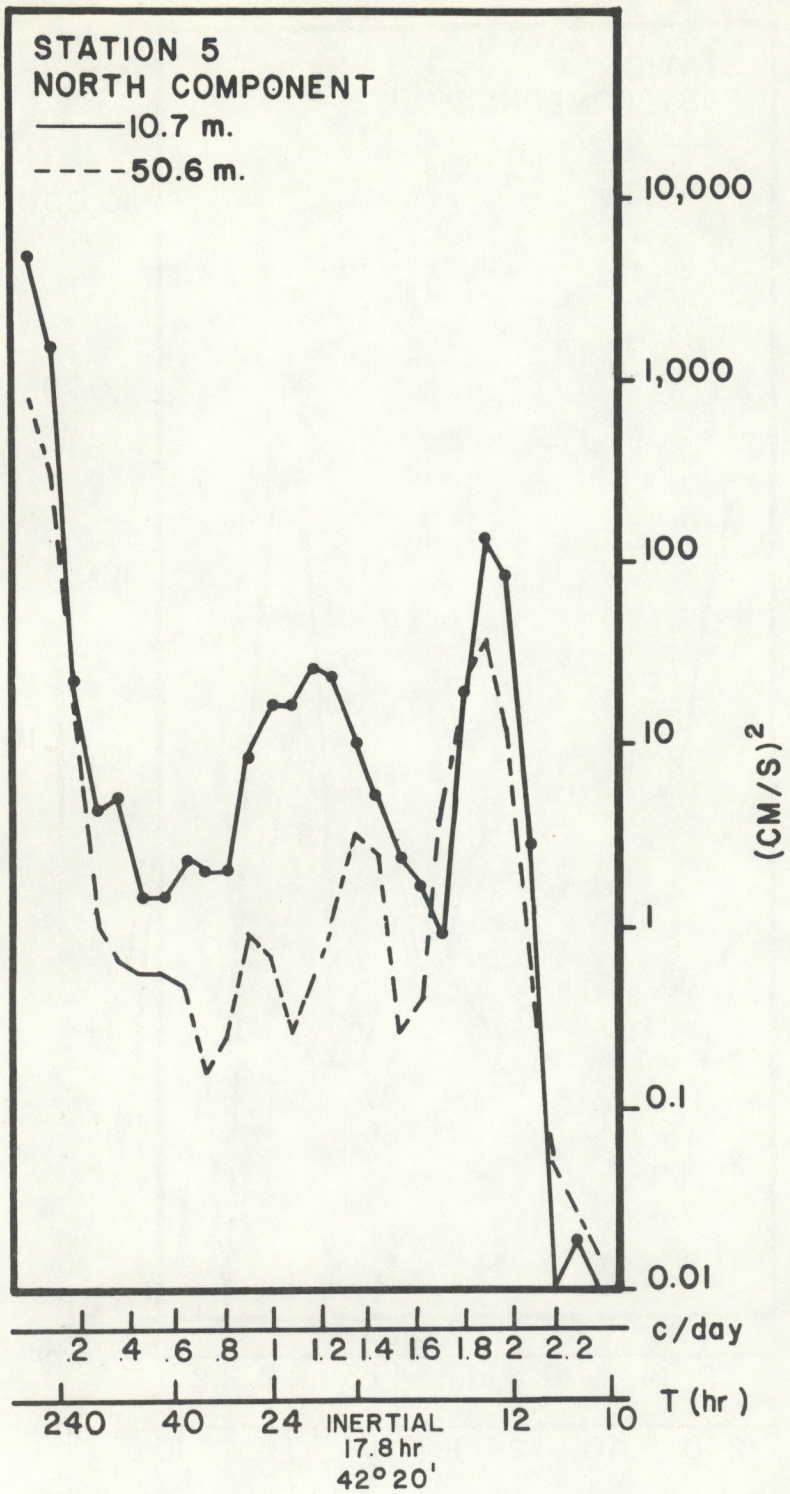

Figure 17. Spectra of north component of current for station 5 at 10.7 and 50.6 m.

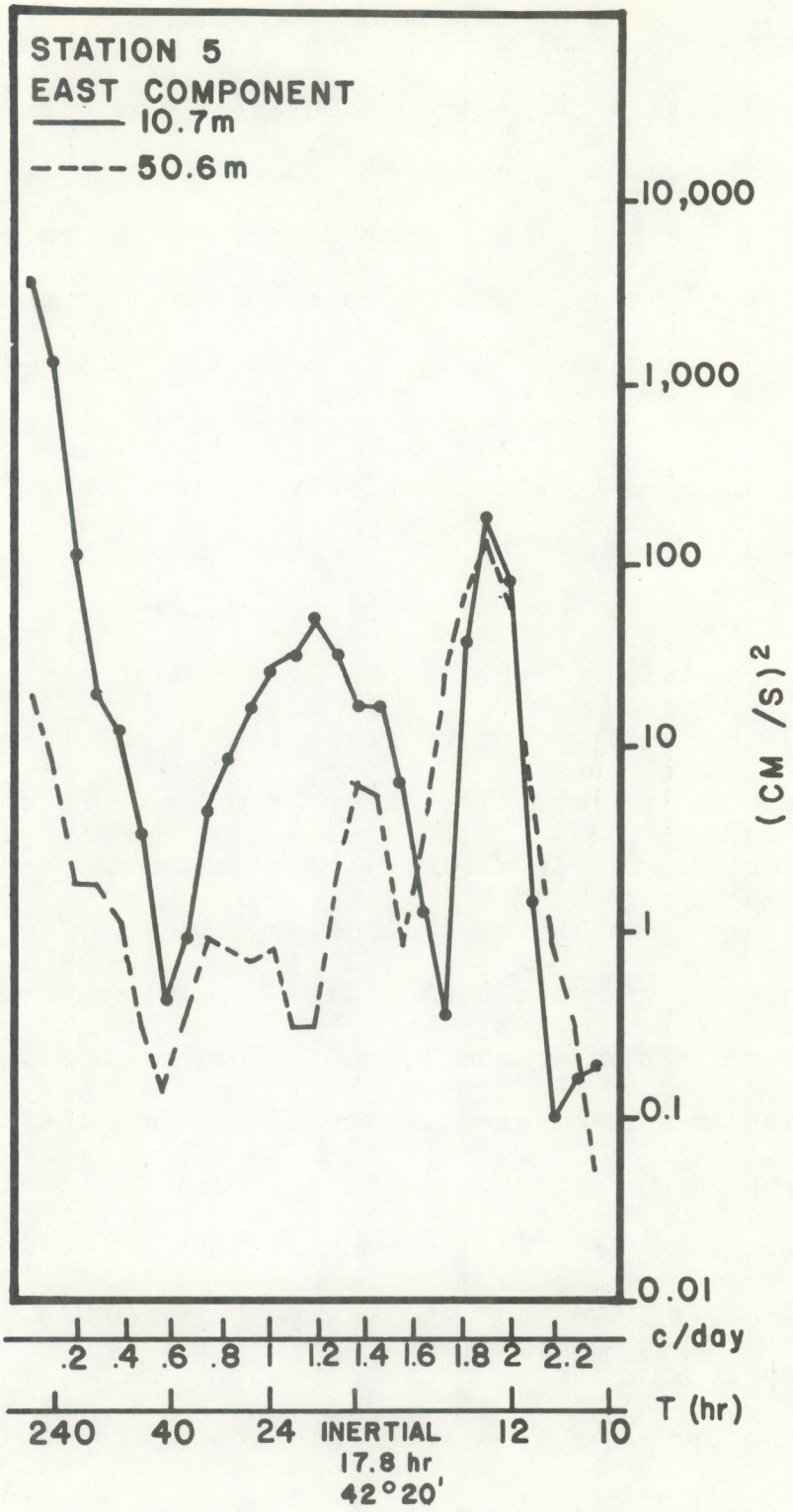

Figure 18. Spectra of east component of current for station 5 at 10.7 and 50.6 m.

of HPV to the total variance for stations A and 5. These characteristics of station 5 data are not clearly duplicated by any of the other stations. However, the total variance decreases with depth in most cases. This can be seen by the much lower energy in the spectra of the deeper sensors in figures 17 and 18. Thus, it seems that any material introduced in the water column beyond stations 5 and B would be dispersed in the water column increasingly by the lower frequencies than would be the case nearer the shore.

4. DROGUE TRACKS

The tracks of the 7- and 12-m drogues are shown in figure 19 and 20. Each point on the track is an observation taken at a specific time. The observation numbers and associated times are listed in table 3. The locations of all current meters are also shown. Following figures 19 and 20 are sequences of current vector fields for each drogue observation. There are 19 for drogue 1 and 29 for drogue 2. Each drogue position and associated vector field show the actual drogue position at the observed time in relation to all the other drogue positions. The current vector fields were constructed from 3-hr lp data that include both low and high frequencies.

By looking at each drogue observation, it can be seen that the drogue movement is not inconsistent with the current vectors; in fact, it is quite clear that the 12-m drogue in figures 20-1 through 20-29 is in phase with the vector at

Table 3.

Times of Drogue Observations for the 7- and 12-m Drogues

Drogue number 1 (7 m), beginning 6-11-73				Drogue number 2 (12 m), beginning 6-11-73					
OBS#	Time	OBS#	Time	OBS#	Time	OBS#	Time	OBS#	Time
1	1100	11	0200	1	1100	11	0100	21	1800
2	1300	12	0300	2	1200	12	0200	22	2100
3	1400	13	0500	3	1300	13	0300	23	2300
4	1600	14	0600	4	1400	14	0500	24	0000
5	1700	15	1000	5	1600	15	0600	25	0100
6	2000	16	1100	6	1700	16	0900	26	0200
7	2200	17	1300	7	2000	17	1100	27	0300
8	2300	18	1400	8	2100	18	1300	28	0400
9	0000	19	1600	9	2300	19	1500	29	0600
10	0100			10	0000	20	1700		

Note: All times have been rounded off to the nearest hour to correspond with hourly current meter data.

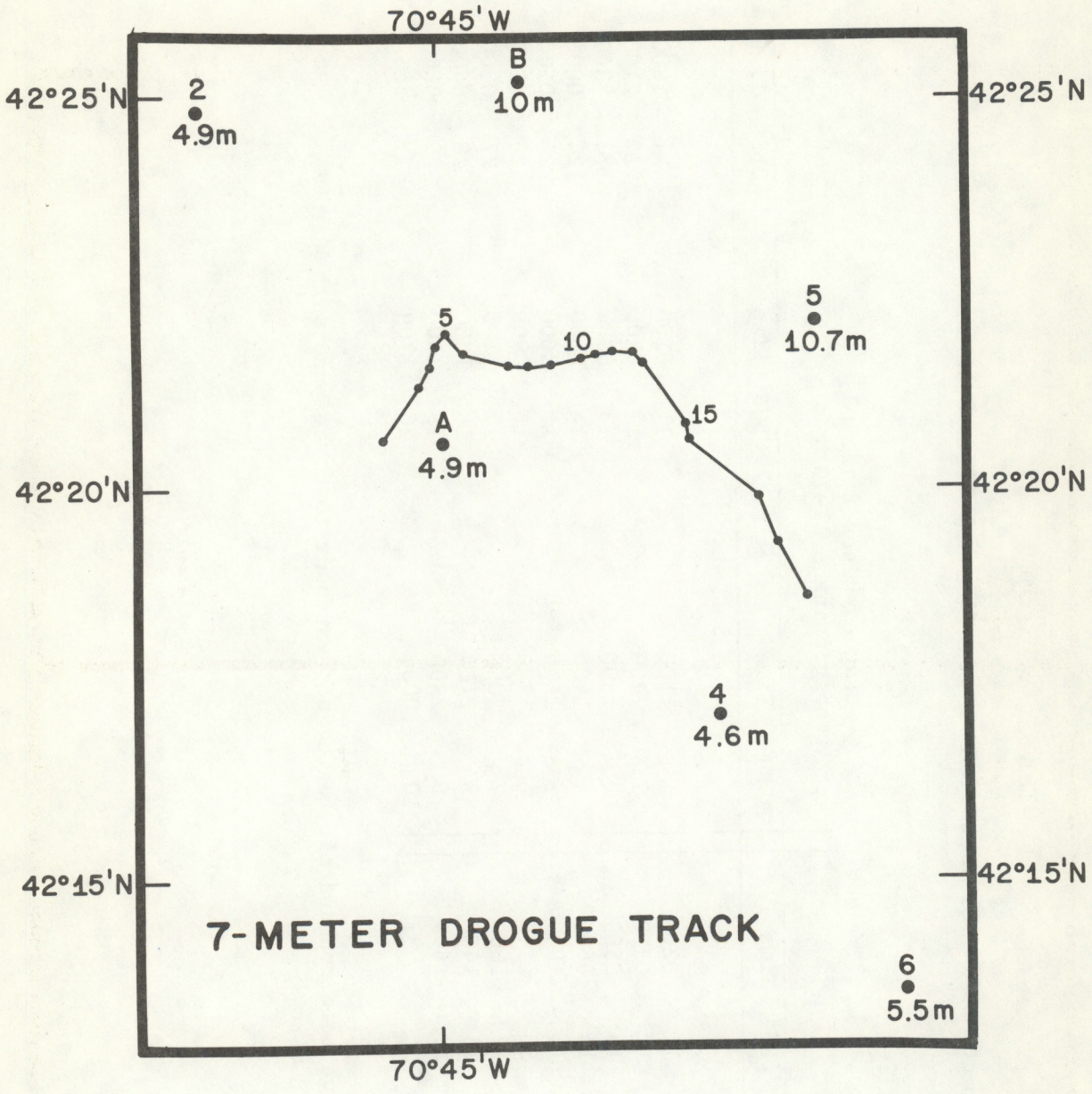

Figure 19. Seven-m drogue track from 1100, June 11, to 1600, June 12; 19-1 through 19-19 are current vectors at the time of drogue position observations.

Figure 19-1.

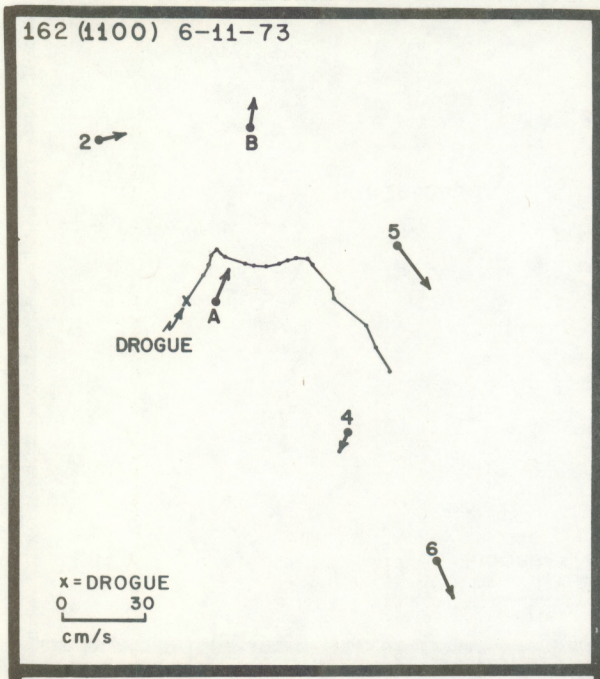

Figure 19-2.

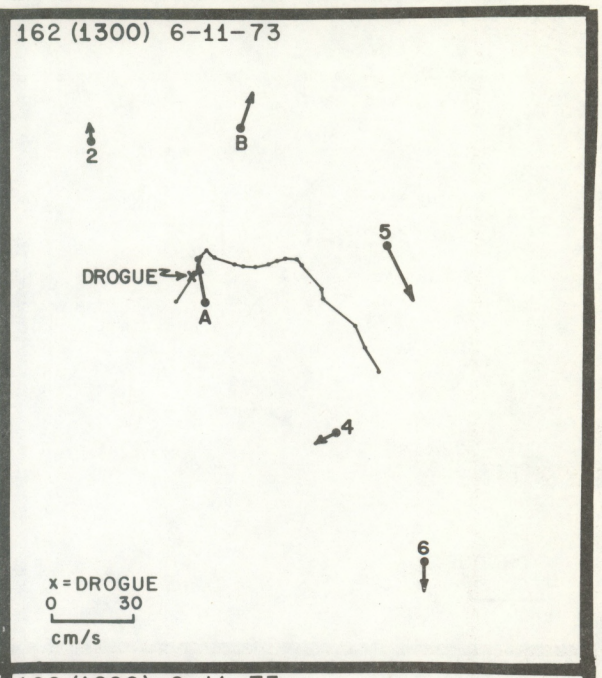

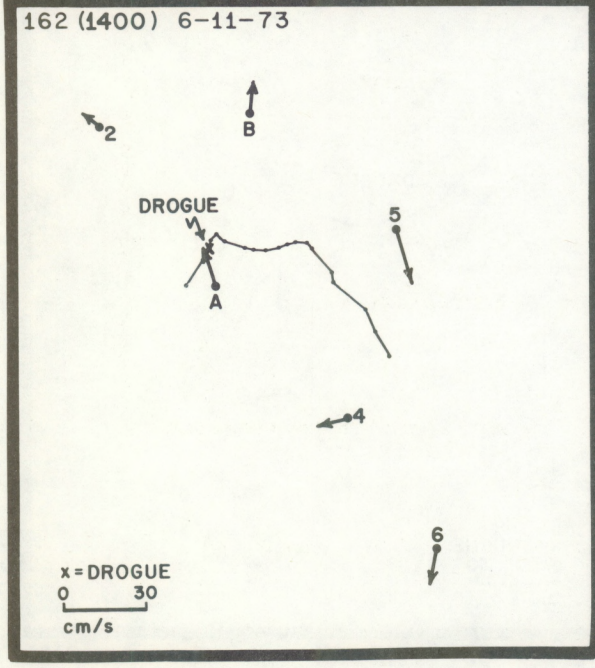

Figure 19-3.

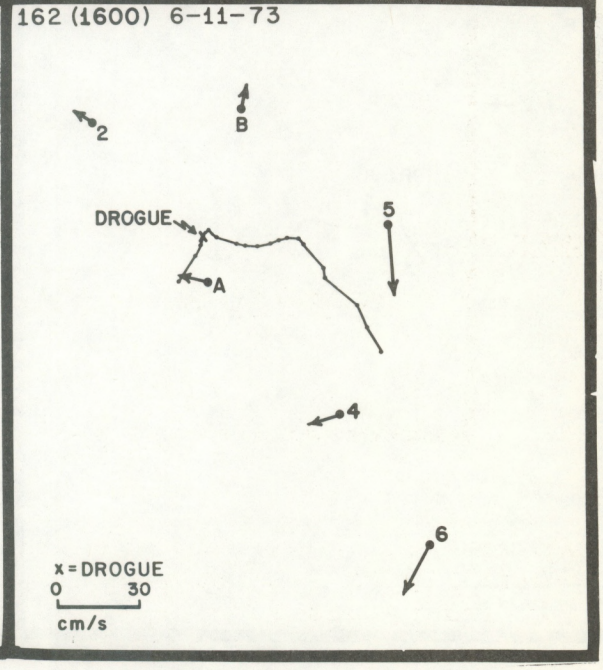

Figure 19-4.

Figure 19-5.

Figure 19-6.

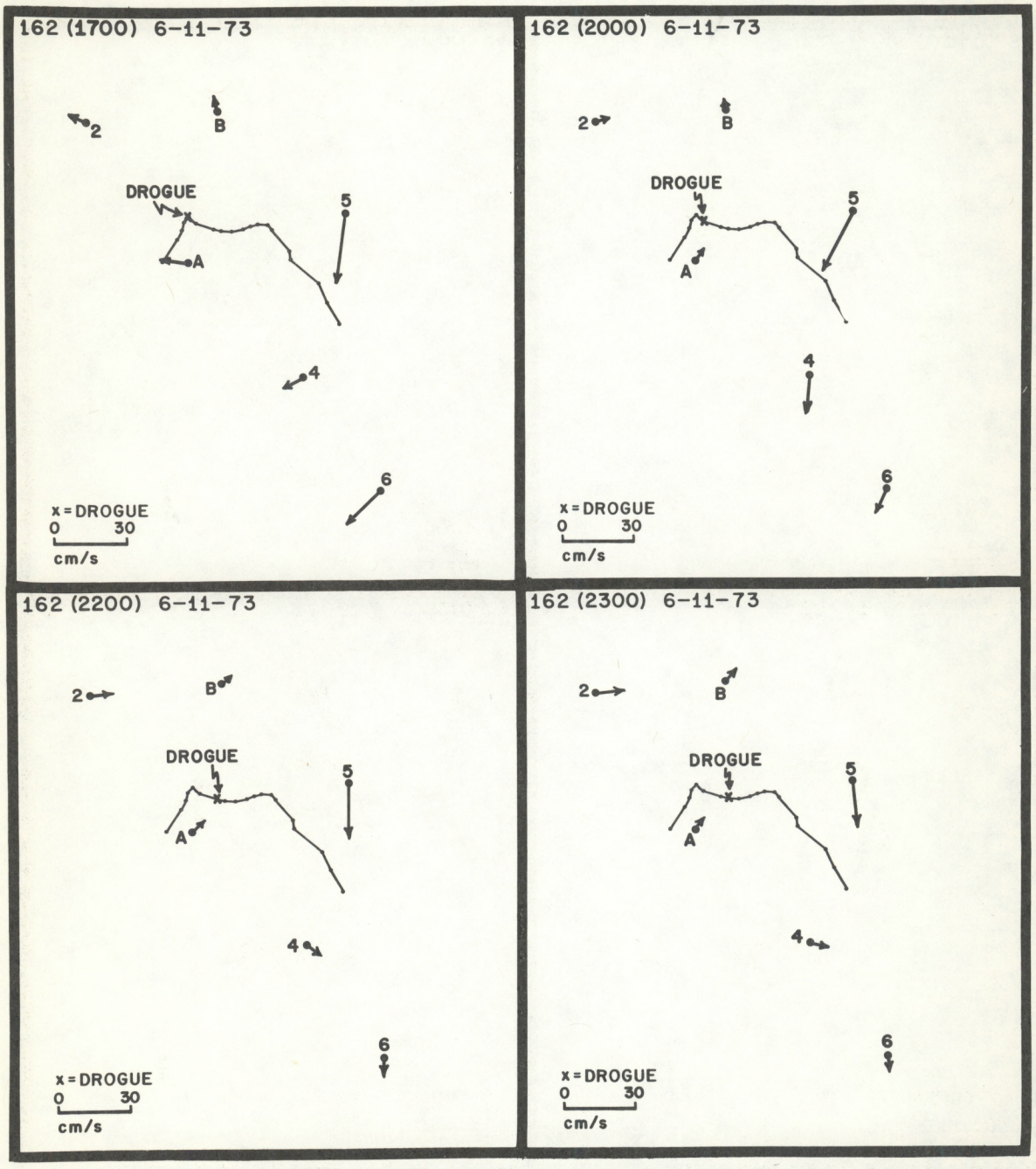

Figure 19-7.

Figure 19-8.

Figure 19-9.

Figure 19-10.

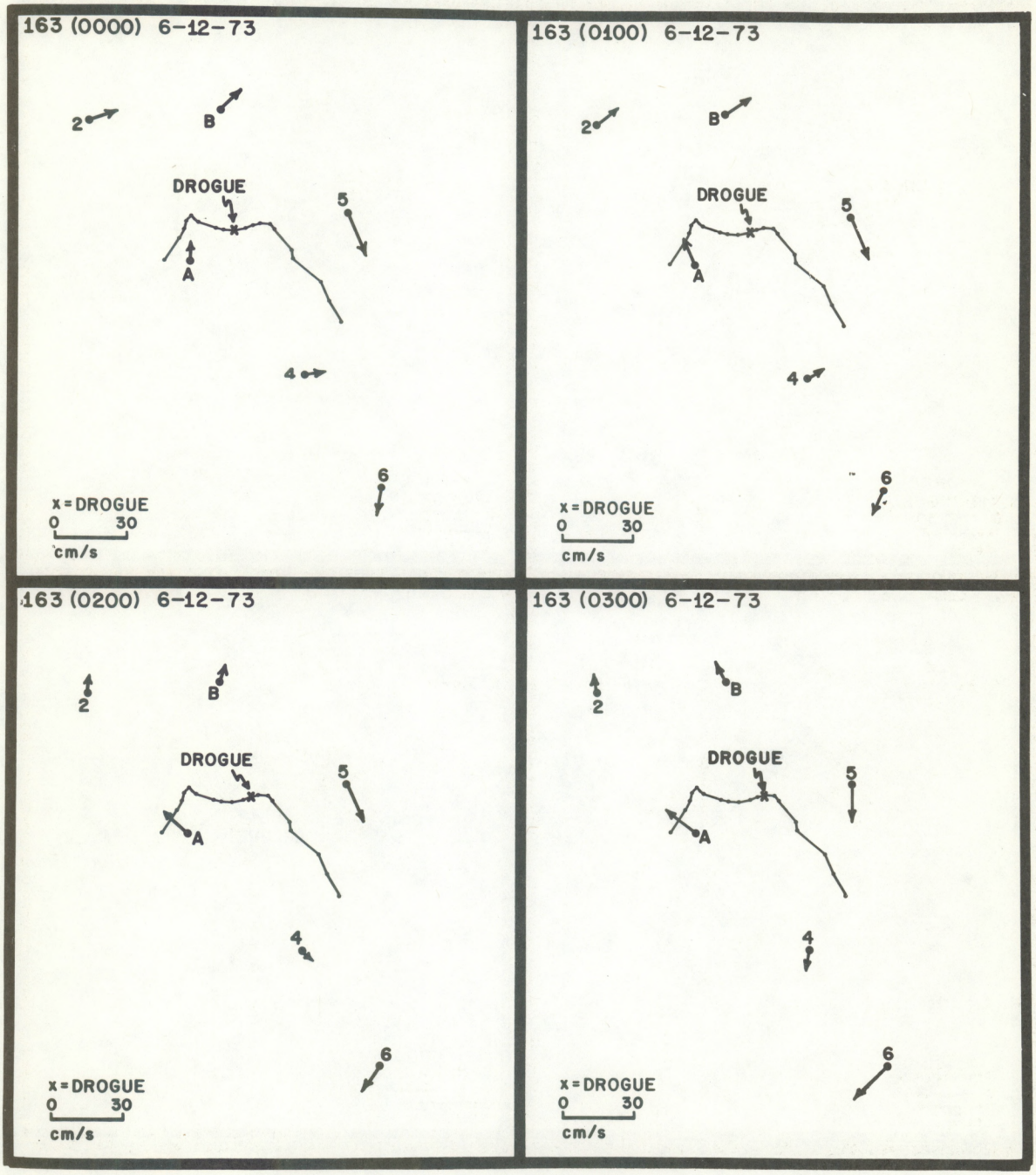

Figure 19-11.

Figure 19-12.

Figure 19-13.

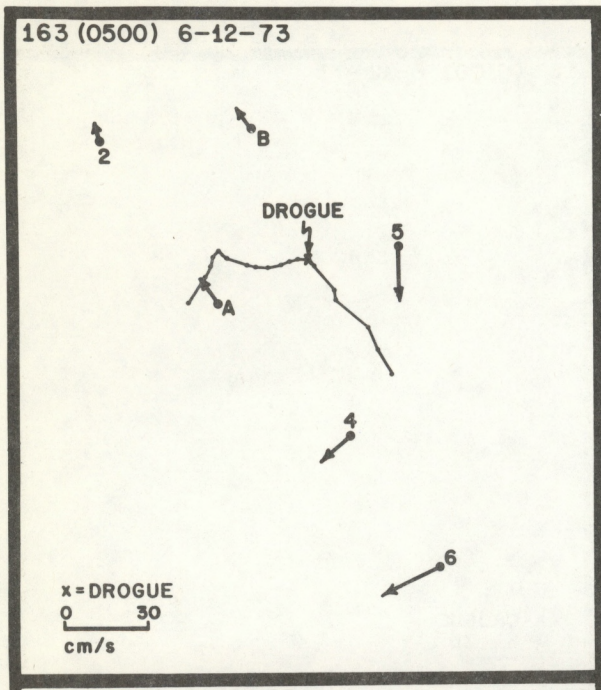

Figure 19-14.

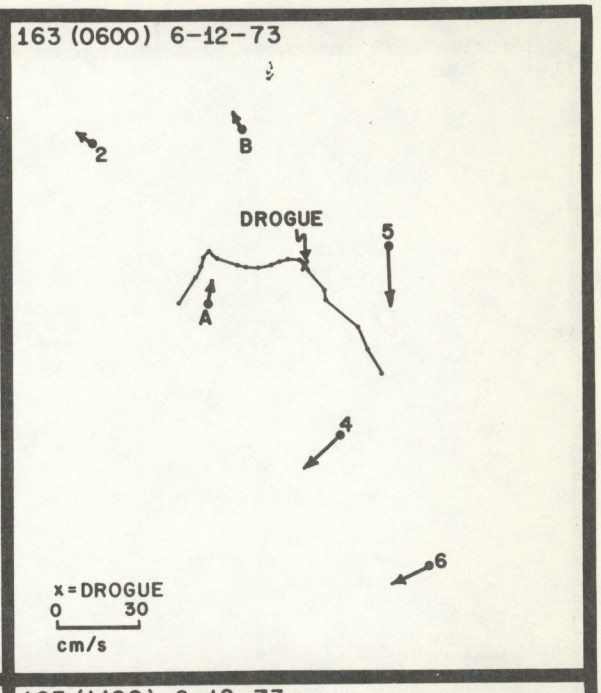

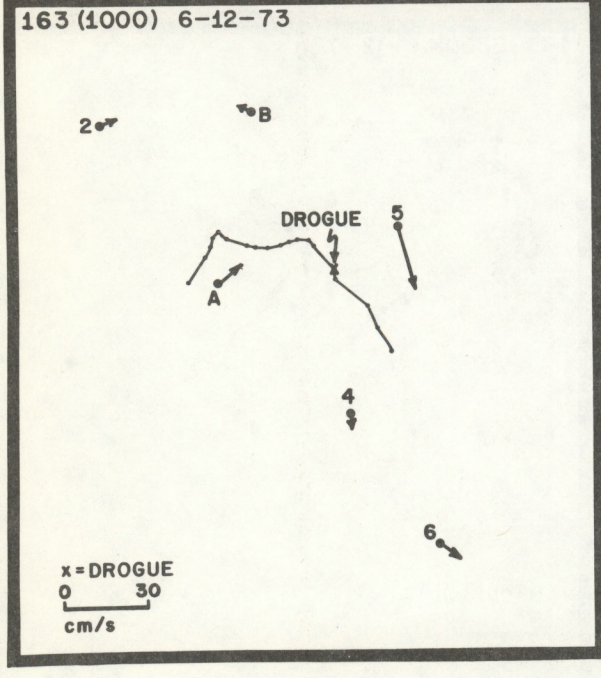

Figure 19-15.

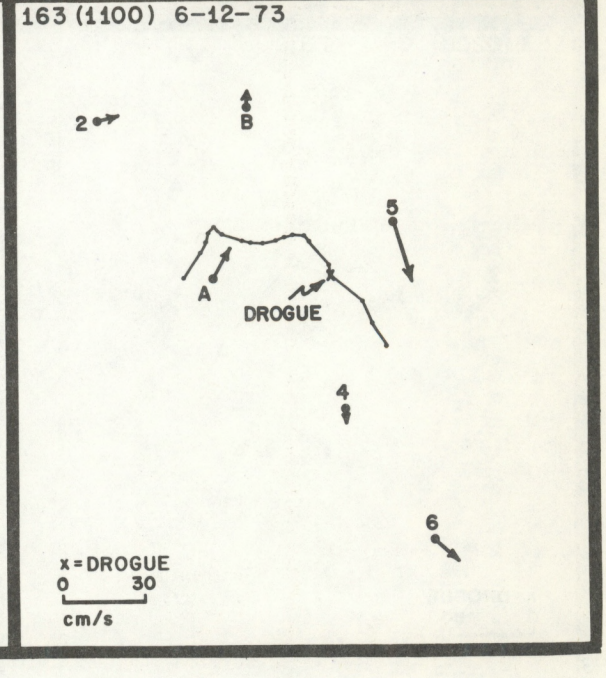

Figure 19-16.

Figure 19-17.

Figure 19-18.

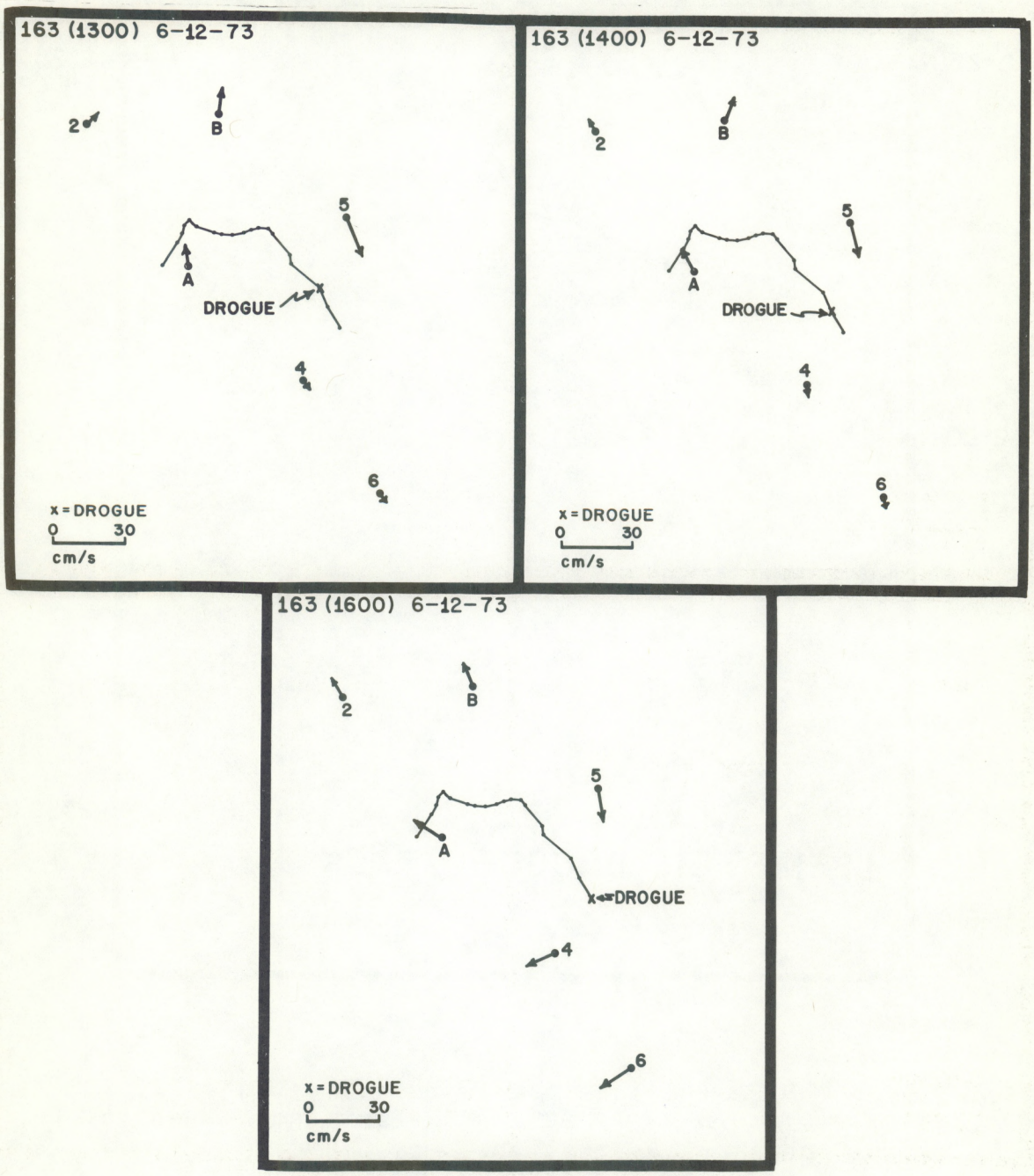

Figure 19-19.

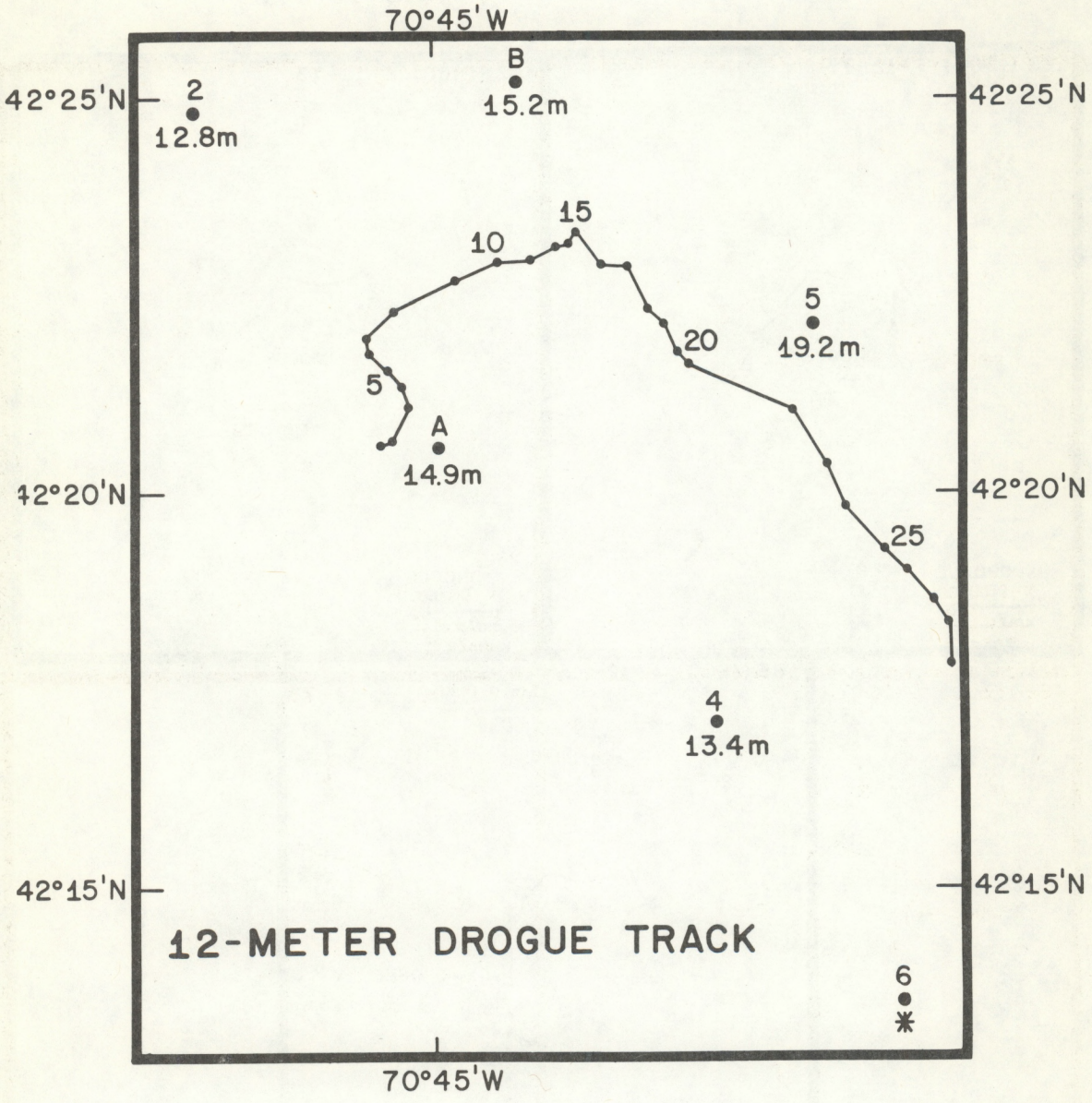

Figure 20. Twelve-m drogue track from 1100, June 11, to 0600, June 13; 20-1 through 20-29 are current vectors at the time of drogue position observation.

Figure 20-1.

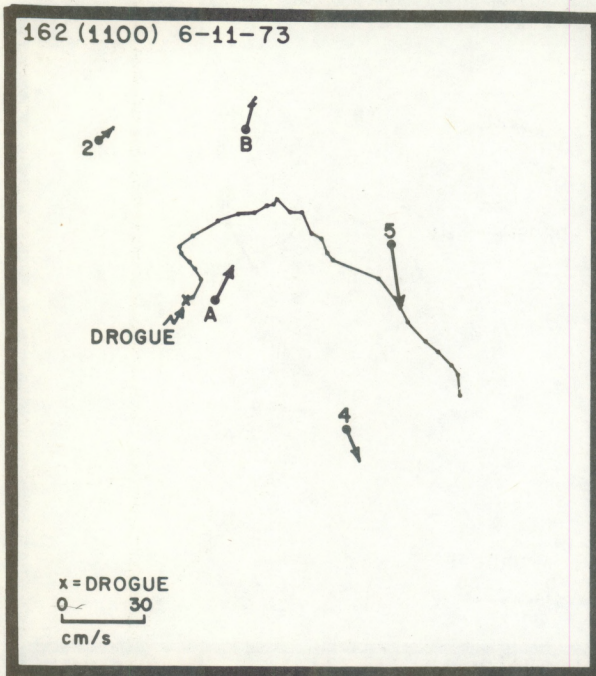

Figure 20-2.

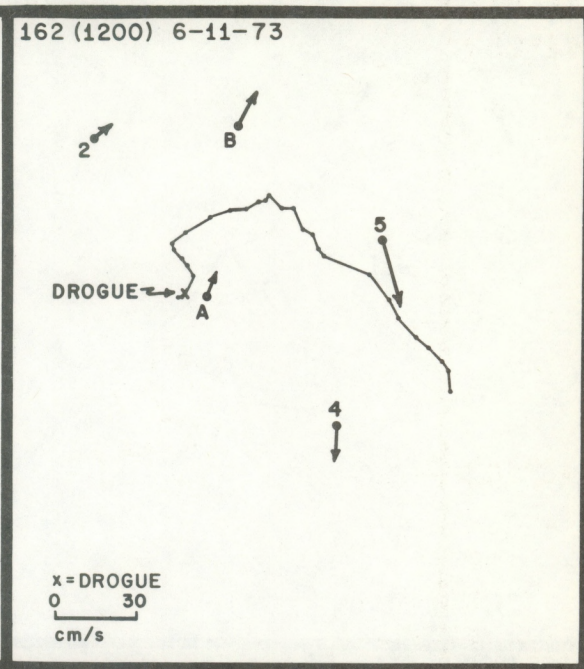

Figure 20-3.

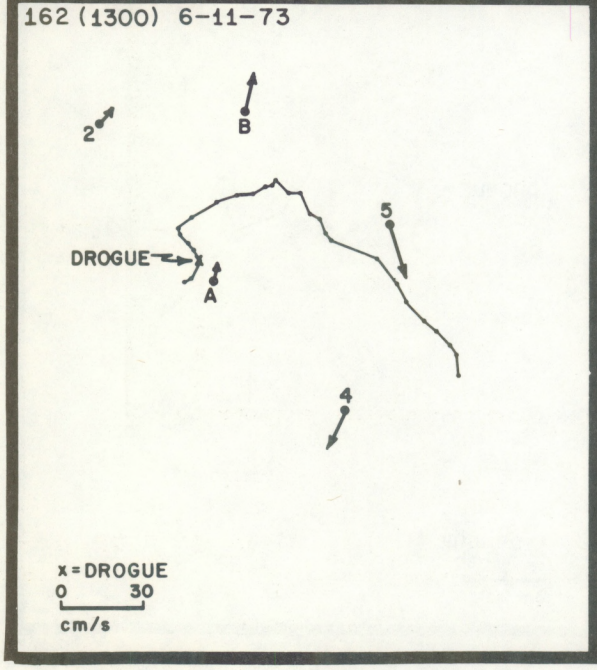

Figure 20-4.

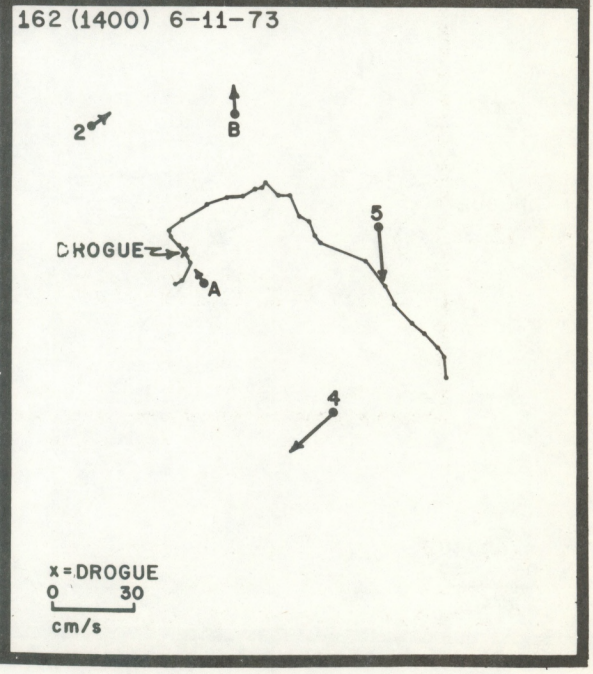

Figure 20-5.

Figure 20-6.

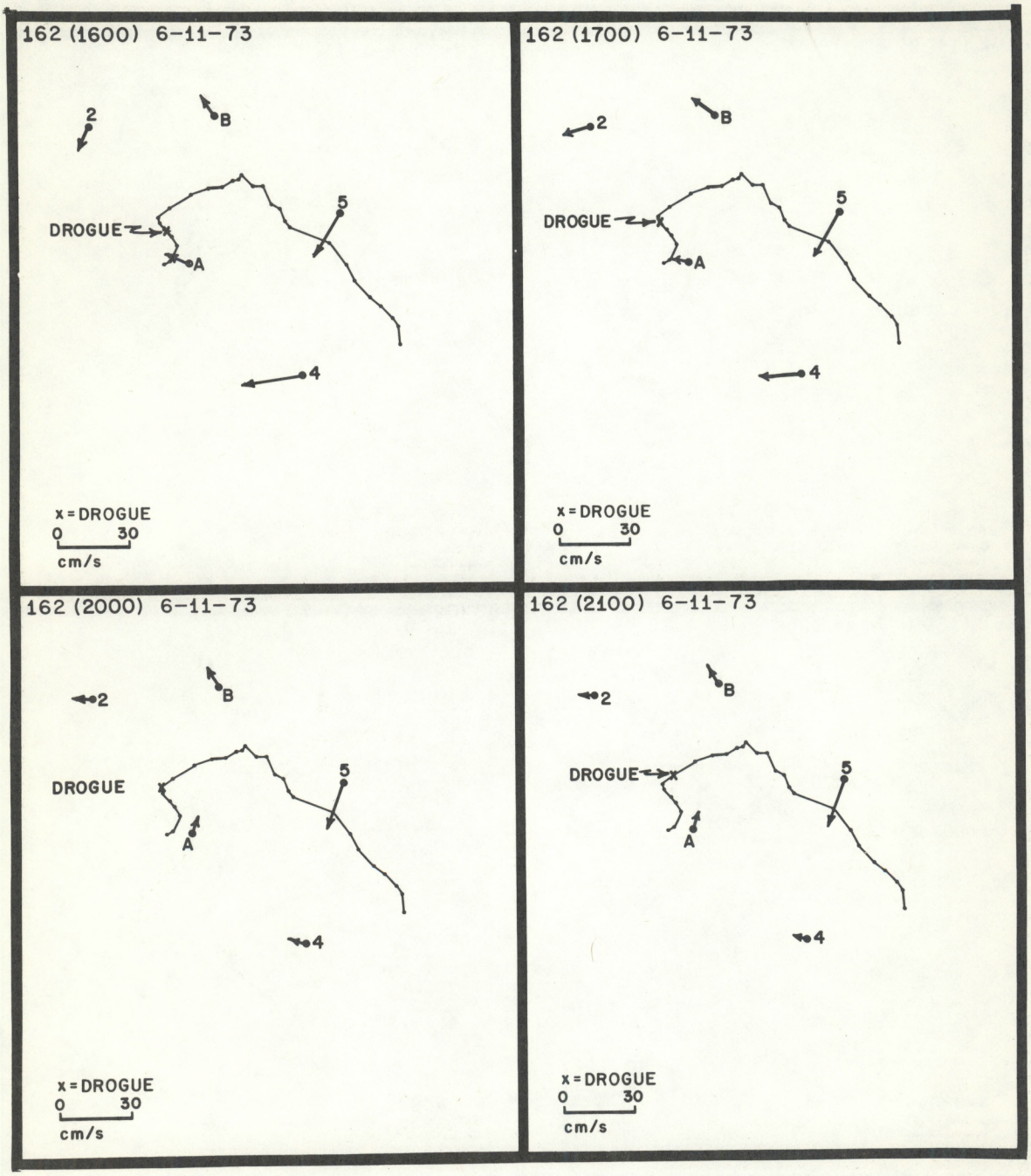

Figure 20-7.

Figure 20-8.

Figure 20-9.

Figure 20-10.

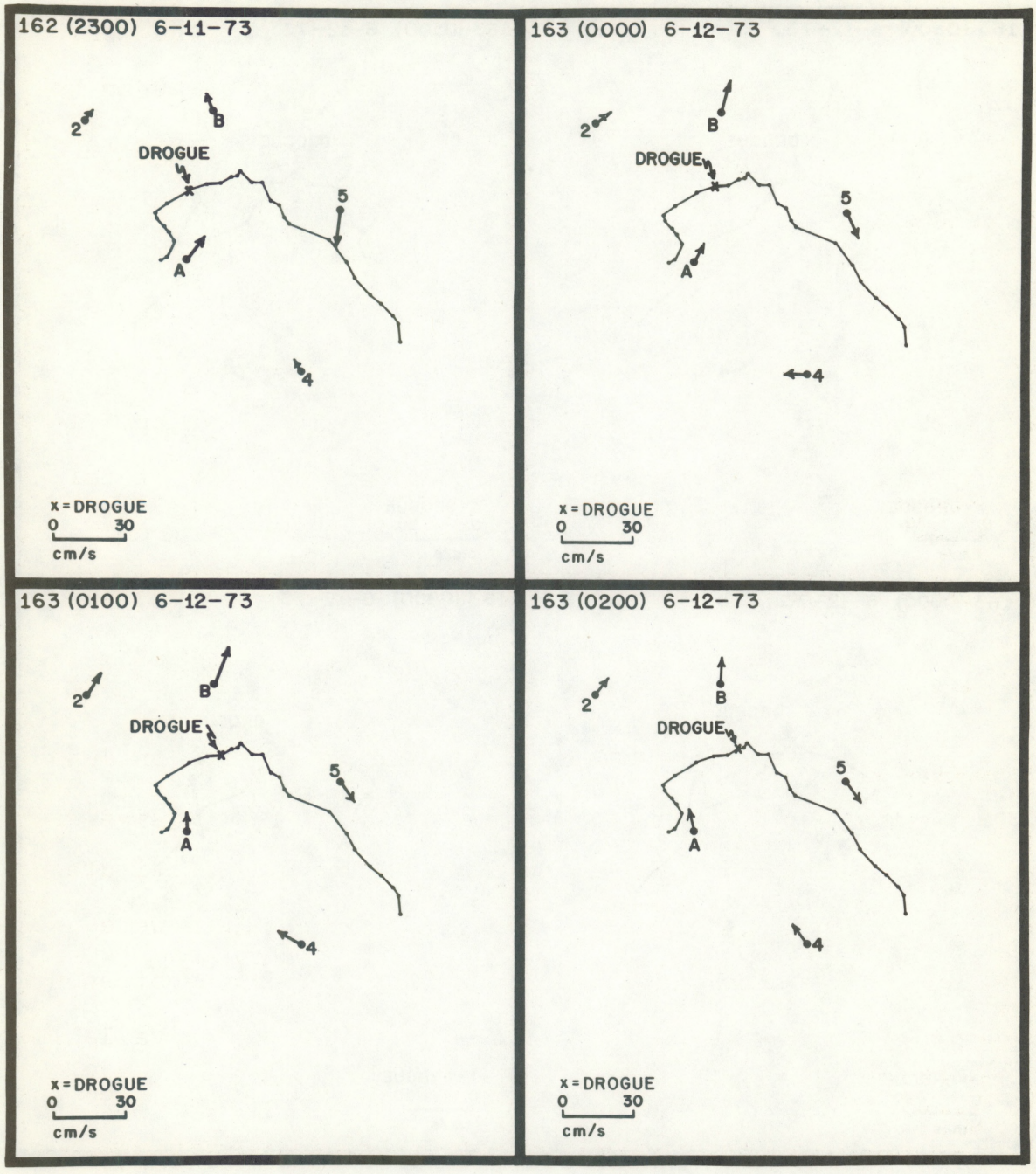

Figure 20-11.

Figure 20-12.

Figure 20-13.

Figure 20-14.

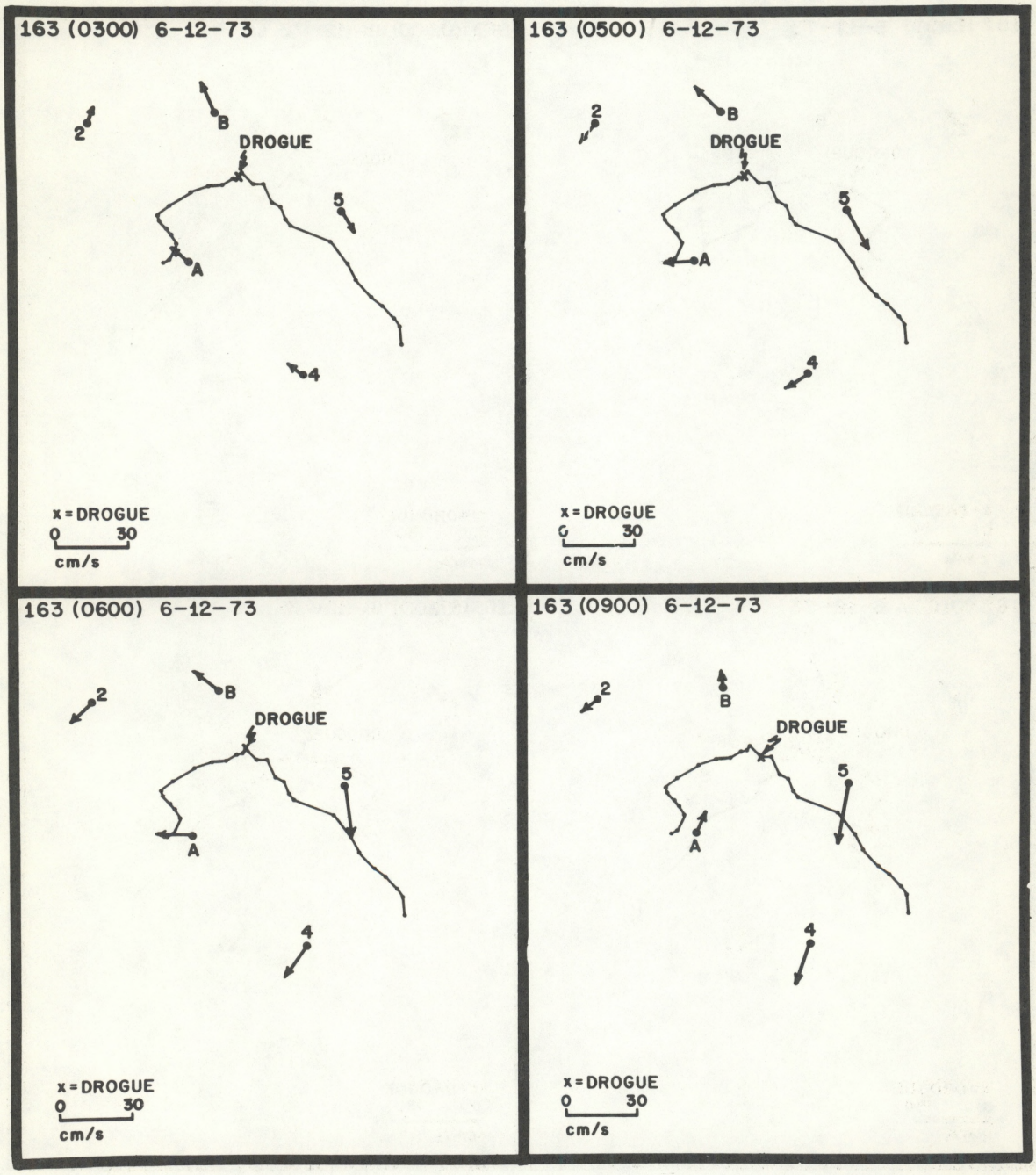

Figure 20-15.

Figure 20-16.

Figure 20-17.

Figure 20-18.

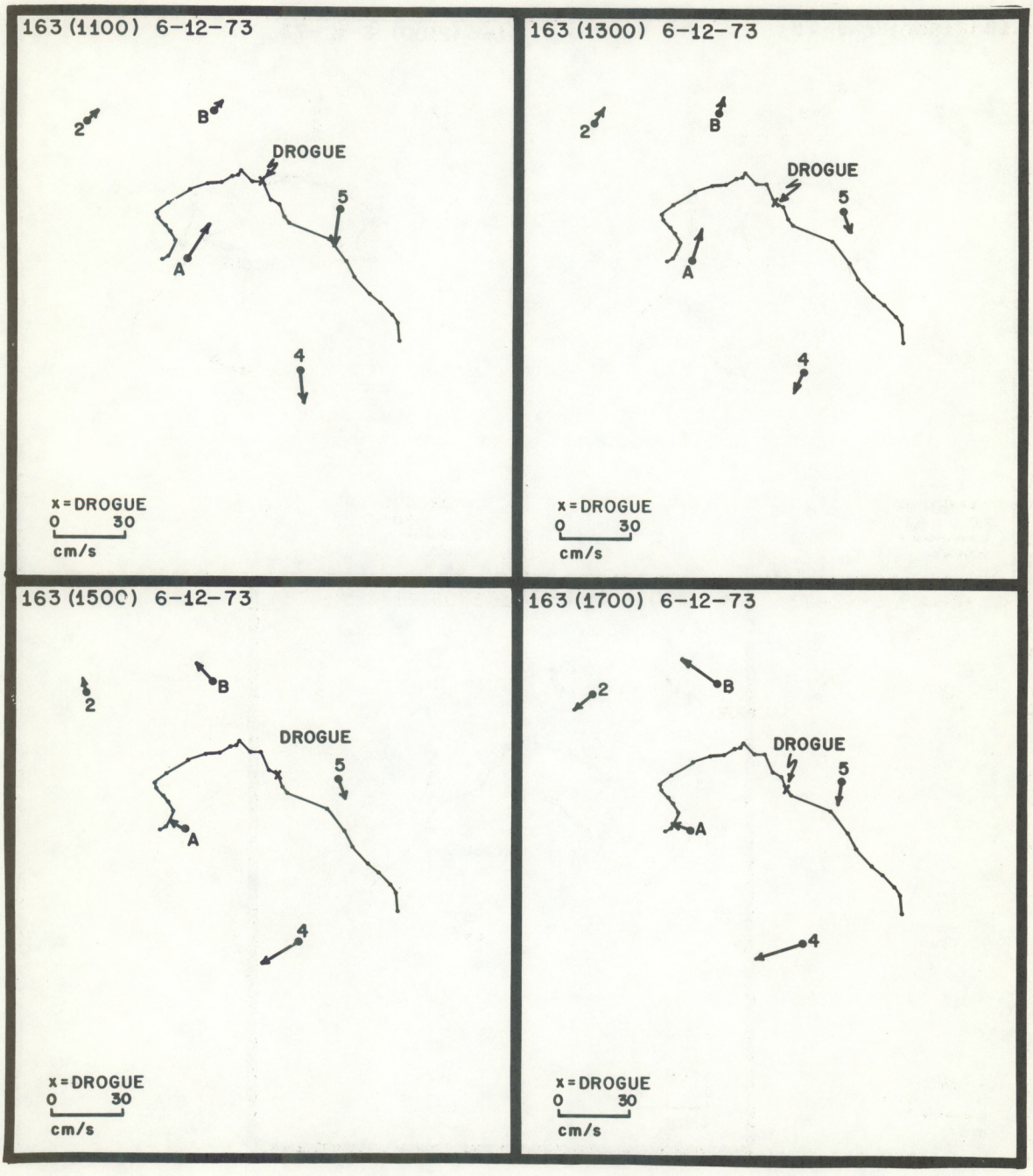

Figure 20-19.

Figure 20-20.

Figure 20-21.

Figure 20-22.

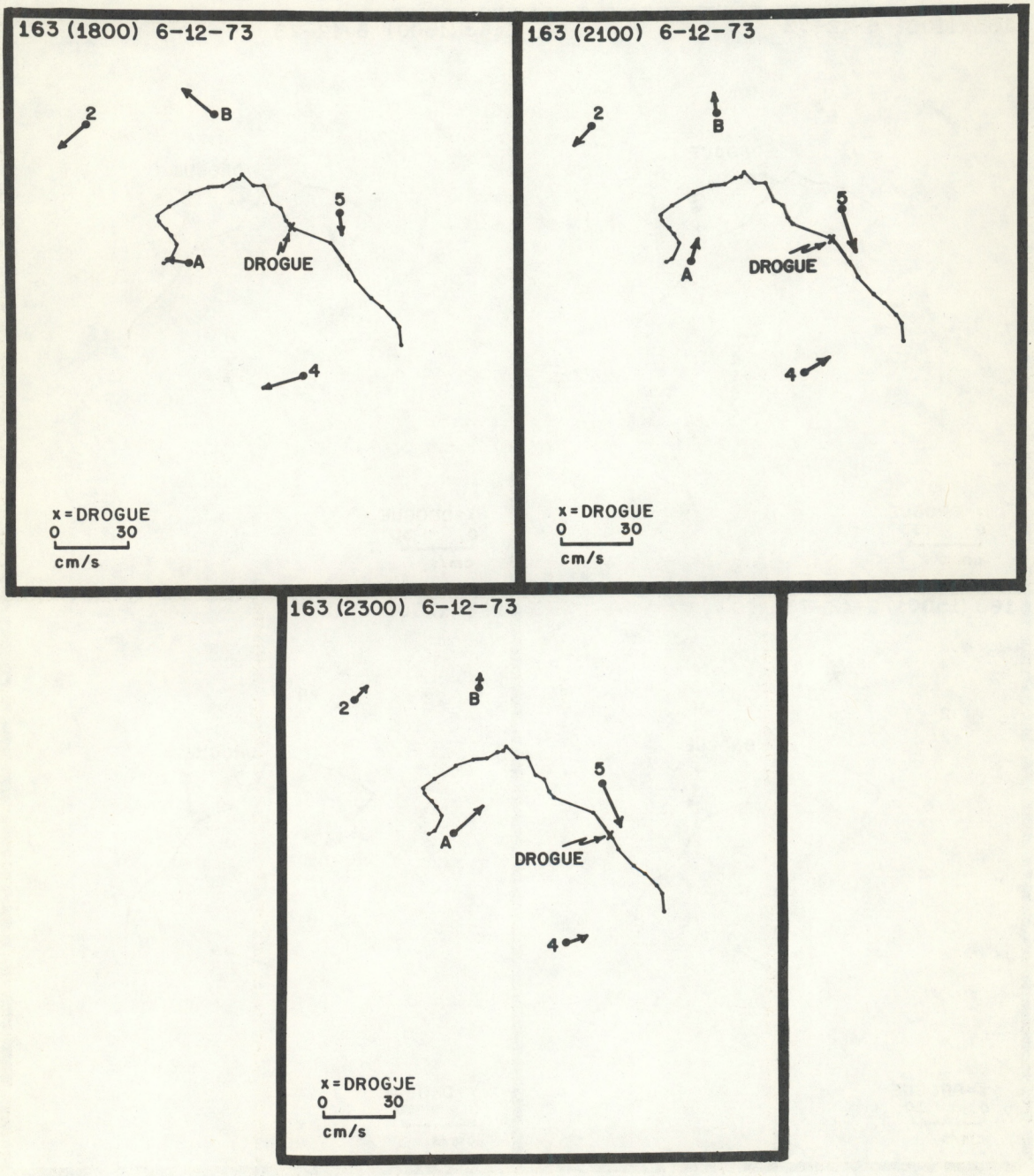

Figure 20-23.

Figure 20-24.

Figure 20-25.

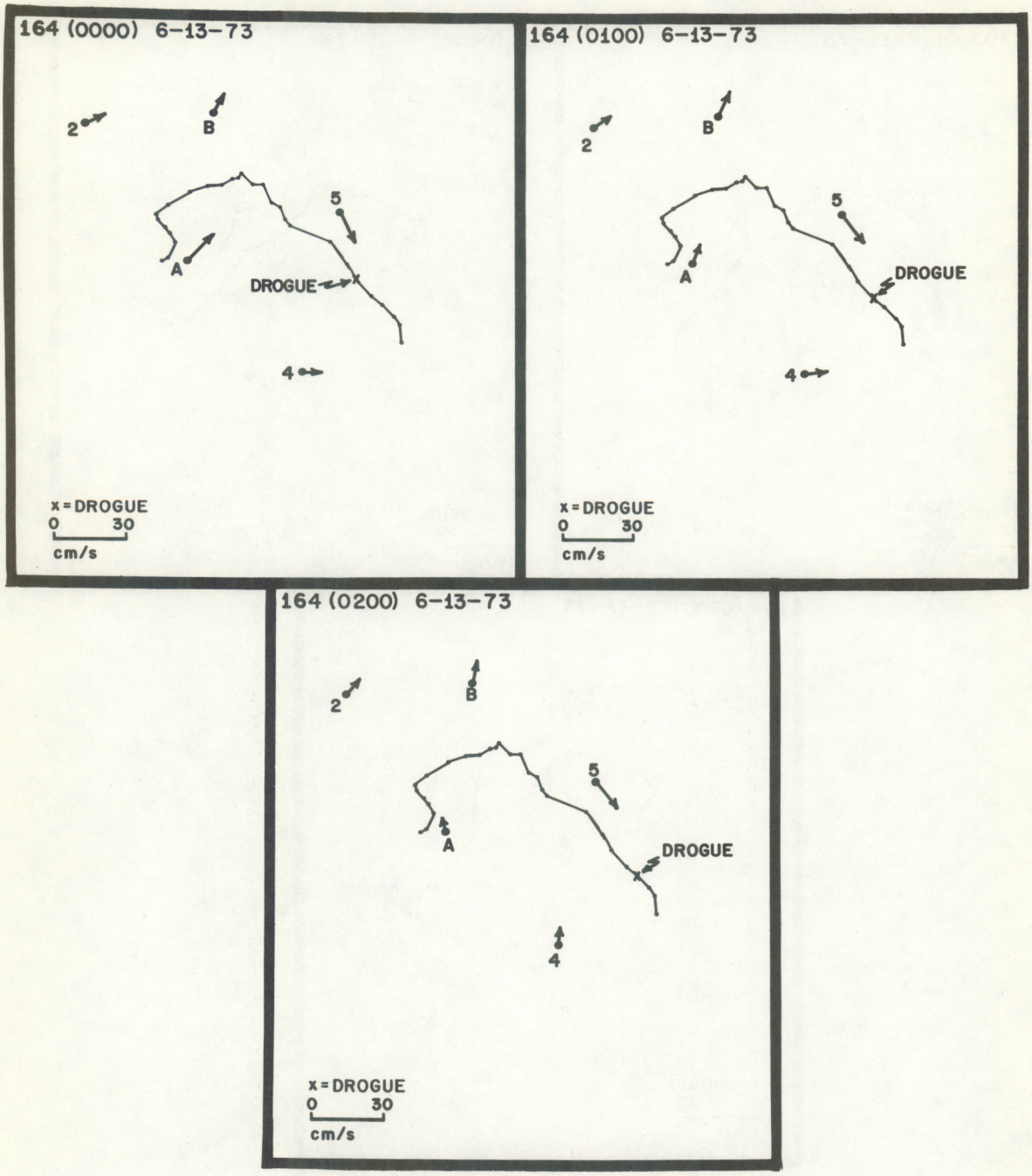

Figure 20-26.

Figure 20-27.

Figure 20-28.

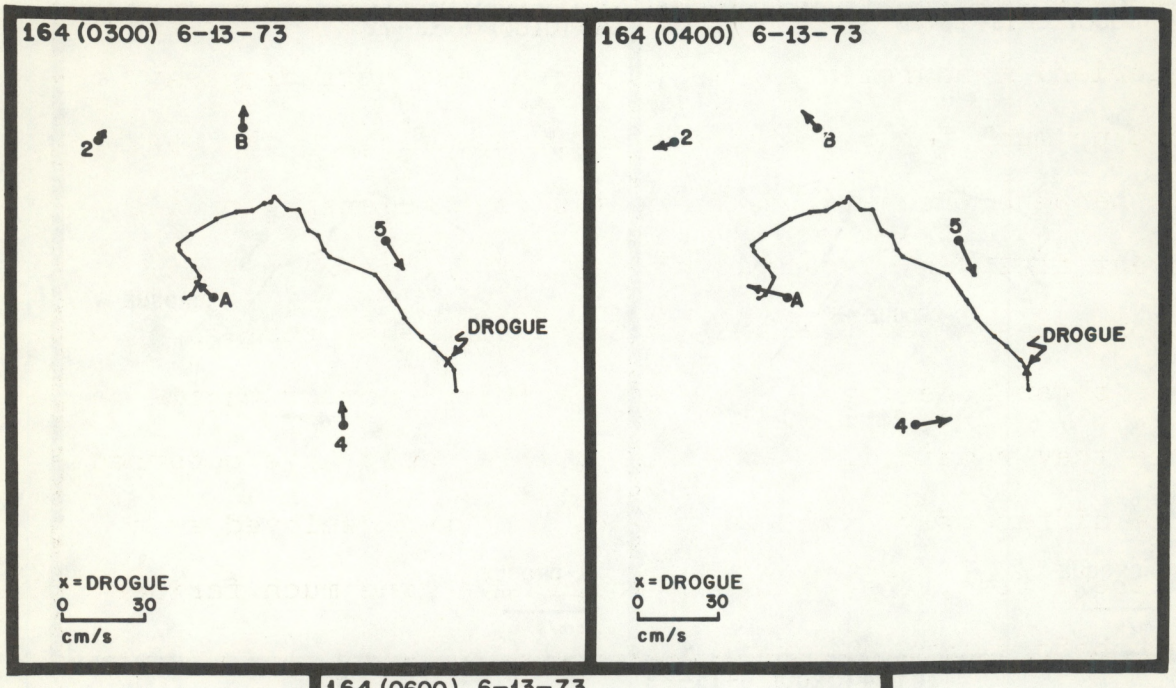

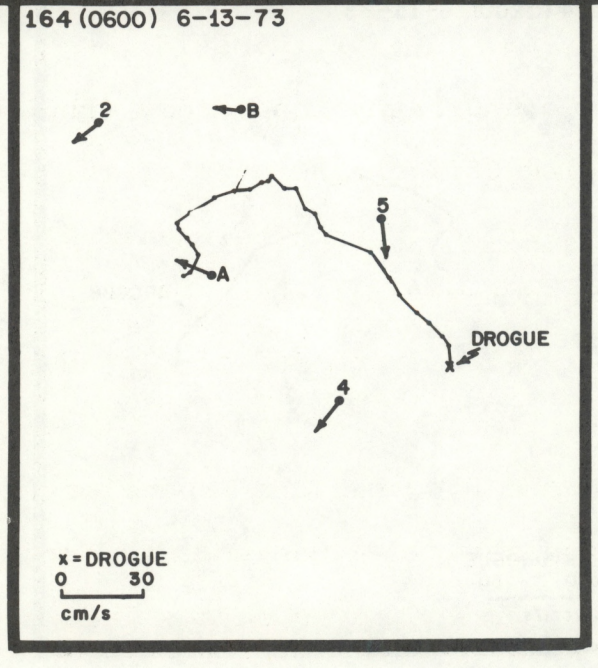

Figure 20-29.

station A while it is near A. As the drogue advances along the track from 20-1 through 20-14, it fluctuates east and then west and then east again in phase with the fixed-point (Eulerian) measurements at A. Ultimately, both drogues wound up much farther offshore and travelling to the south. This happened because of the spatial inhomogeneity of the current field in Massachusetts Bay. The east-west tidal motion transported the drogues far enough east through a sharp shear zone into a southerly flowing current regime where they remained. Conceivably, this could have occurred quite differently. If the drogues had been deployed at a different time, they probably would have gone much farther north before turning south.

5. ACKNOWLEDGMENTS

The Physical Oceanography Laboratory (PhOL) of AOML thanks the Commanding Officer and crew of the U.S. Coast Guard buoy tender Whiteheath for their valuable assistance during deployment and retrieval of the current meter moorings.

Appreciation is also expressed to Alan Herman, PhOL Systems Programmer, for translating the EG&G current meter data types, and to the R.M. Parsons Laboratory at MIT for providing the drogue data in a convenient format to facilitate comparison with the current meter data. Thanks is also extended to Rich Boehmer, State of Massachusetts, Department of Water Resources, for furnishing the Boston Lightship wind data.

6. REFERENCES

Magas, A. P. (1973): Oceanographic Report: NOMES Project Massachusetts Bay, Massachusetts, for NOAA by EG&G Environmental Equipment Division, Waltham, Mass.

☆GPO 1975—677-241/1265 REGION NO. 8

ENVIRONMENTAL RESEARCH LABORATORIES

The mission of the Environmental Reasearch Laboratories is to study the oceans, inland waters, the lower and upper atmosphere, the space environment, and the earth, in search of the understanding needed to provide more useful services in improving man's prospects for survival as influenced by the physical environment. Laboratories contributing to these studies are:

Atlantic Oceanographic and Meteorological Laboratories (AOML): Geology and geophysics of ocean basins and borders, oceanic processes, sea-air interactions and remote sensing of ocean processes and characteristics (Miami, Florida).

Pacific Marine Environmental Laboratory (PMEL): Environmental processes with emphasis on monitoring and predicting the effects of man's activities on estuarine, coastal, and near-shore marine processes (Seattle, Washington).

Great Lakes Environmental Research Laboratory (GLERL): Physical, chemical, and biological, limnology, lake-air interactions, lake hydrology, lake level forecasting, and lake ice studies (Ann Arbor, Michigan).

Atmospheric Physics and Chemistry Laboratory (APCL): Processes of cloud and preciptation physics; chemical composition and nucleating substances in the lower atmosphere; and laboratory and field experiments toward developing feasible methods of weather modification.

Air Resources Laboratories (ARL): Diffusion, transport, and dissipation of atmospheric contaminants; development of methods for prediction and control of atmospheric pollution; geophysical monitoring for climatic change (Silver Spring, Maryland).

Geophysical Fluid Dynamics Laboratory (GFDL): Dynamics and physics of geophysical fluid systems; development of a theoretical basis, through mathematical modeling and computer simulation, for the behavior and properties of the atmosphere and the oceans (Princeton, New Jersey).

National Severe Storms Laboratory (NSSL): Tornadoes, squall lines, thunderstorms, and other severe local convective phenomena directed toward improved methods of prediction and detection (Norman, Oklahoma).

Space Environment Laboratory (SEL): Solar-terrestrial physics, service and technique development in the areas of environmental monitoring and forecasting.

Aeronomy Laboratory (AL): Theoretical, laboratory, rocket, and satellite studies of the physical and chemical processes controlling the ionosphere and exosphere of the earth and other planets, and of the dynamics of their interactions with high-altitude meteorology.

Wave Propagation Laboratory (WPL): Development of new methods for remote sensing of the geophysical environment with special emphasis on optical, microwave and acoustic sensing systems.

Marine EcoSystem Analysis Program Office (MESA): Plans and directs interdisciplinary analyses of the physical, chemical, geological, and biological characteristics of selected coastal regions to assess the potential effects of ocean dumping, municipal and industrial waste discharges, oil pollution, or other activity which may have environmental impact.

Weather Modification Program Office (WMPO): Plans and directs ERL weather modification research activities in precipitation enhancement and severe storms mitigation and operates ERL's research aircraft.

NATIONAL OCEANIC AND ATMOSPHERIC ADMINISTRATION
BOULDER, COLORADO 80302

USCOMM - ERL